PHYSICAL REVIEW B **82**, 184207 (2010)

Temperature-induced crossovers in the static roughness of a one-dimensional interface

Elisabeth Agoritsas,[1,*] Vivien Lecomte,[1,2] and Thierry Giamarchi[1]
[1]*DPMC-MaNEP, University of Geneva, 24 Quai Ernest-Ansermet, 1211 Geneva 4, Switzerland*
[2]*Laboratoire de Probabilités et Modèles Aléatoires (CNRS UMR 7599), Université Paris Diderot, 2 Place Jussieu, 75251 Paris Cedex 05, France*
(Received 20 August 2010; published 22 November 2010)

At finite temperature and in presence of disorder, a one-dimensional elastic interface displays different scaling regimes at small and large lengthscales. Using a replica approach and a Gaussian variational method (GVM), we explore the consequences of a finite interface width ξ on the small-lengthscale fluctuations. We compute analytically the static roughness $B(r)$ of the interface as a function of the distance r between two points on the interface. We focus on the case of short-range elasticity and random-bond disorder. We show that for a finite width ξ two temperature regimes exist. At low temperature, the expected thermal and random-manifold regimes, respectively, for small and large scales, connect via an intermediate "modified" Larkin regime, that we determine. This regime ends at a temperature-independent characteristic "Larkin" length. Above a certain characteristic temperature that we identify, this intermediate regime disappears. The thermal and random-manifold regimes connect at a single crossover lengthscale, that we compute. This is also the expected behavior for zero width. Using a directed polymer description, we also study via a second GVM procedure and generic scaling arguments, a modified toy model that provides further insights on this crossover. We discuss the relevance of the two GVM procedures for the roughness at large lengthscale in those regimes. In particular, we analyze the scaling of the temperature-dependent prefactor in the roughness $B(r) \sim T^{2p} r^{2\zeta}$ and its corresponding *thorn* exponent p. We briefly discuss the consequences of those results for the quasistatic creep law of a driven interface, in connection with previous experimental and numerical studies.

DOI: 10.1103/PhysRevB.82.184207 PACS number(s): 05.20.−y, 05.40.−a, 68.35.Ct, 75.60.Ch

I. INTRODUCTION

Almost everyone has already unwittingly spilt coffee on her/his work table and observed the inexorable progression of the liquid into her/his favorite article. However inconvenient may be the consequences of such a simple home experiment, it shares in fact a lot of common physical features with a variety of systems and phenomena ranging from ferromagnetic[1,2] and ferroelectric[3,4] domain walls (DWs), to growth surfaces,[5] contact line in wetting experiments,[6,7] or crack propagation in paper.[8] All those systems display different coexisting phases separated by an interface, whose shape and dynamics are determined from two competing tendencies: the elastic cost of the interface which tends to flatten it while disorder in the environment induces deformations adapting the interface to the local energetic valleys and hills.

To describe these phenomena, a successful theoretical approach is that of disordered elastic systems[9,10] (DES), in which the bulk details of the interface are summarized in its mere position, seen as a fluctuating manifold whose energy is the sum of elastic and disorder contributions. Such a description also encompasses periodic systems such as charge density waves[11,12] or vortex lattices[13] occurring in type-II superconductors. This approach accounts for a complex free-energy landscape which exhibits metastability and explains the dynamical glassy properties—such as hysteresis, creep or aging—observed in experimental realizations. Such systems display similar features independently of the scale at which they are observed: in other words, they present ranges of scale on which they are statistically scale invariant.[14] A simple way to characterize this property is to study the *roughness* of the interface [denoted $B(r)$], defined as the variance of the relative displacements of the manifold at a given lengthscale r. Scale invariance translates into having the roughness behaving as a power law $B(r) \sim r^{2\zeta}$ characterized by a roughness exponent ζ.

In addition to its direct experimental relevance, e.g., in ferromagnetic domain walls, the one-dimensional (1D) interface shares many universal features with other distinct physical problems, such as the directed polymer (DP) in random media (for reviews, see Refs. 15 and 16), the noisy Burgers' equation in hydrodynamics,[17,18] or bosons with attractive hardcore interaction in one dimension.[19] These systems are all falling in the so-called Kardar-Parisi-Zhang (KPZ) class.[20,21] This problem has now been studied for many decades, the attention being focused on the large-scale—or so-called "random-manifold" (RM)—properties of the roughness: many approaches have been used to establish the nontrivial exponent $\zeta_{\mathrm{RM}}=2/3$ for $B(r) \sim r^{2\zeta}$ in the large r limit, ranging from dynamical renormalization group,[17,22] to hidden symmetries[23] and Bethe Ansatz computations.[19]

In spite of the versatility of the previous studies, there has been a recent uprise of interest in different directions: from a mathematical point of view it is only very recently[24] that the 2/3 RM exponent has been proven, the method itself making the link with another class of systems—transport models known as asymmetric exclusion processes. Besides, in a recent series of works in the mathematics[25,26] and physics[27,28] communities, it has been shown that the free-energy distribution for the polymer end point is obtained from the Tracy-Widom distribution, when the random potential is delta correlated. Similarly, another interesting and related question which seems to have been neglected up to recently is the role of temperature in the large-scale behavior of the roughness:

although physically one could *a priori* expect the roughness to be temperature independent at large lengthscales, since it is dominated by the disorder, it happens that scaling arguments show this shall not be the case at small enough disorder correlation length ξ, and that there is a subtle interplay between low temperature and small ξ limits.[28,29]

Despite these recent progresses several questions remain. In particular, in these works, the width of the interface or the disorder correlation length ξ is assumed to be zero. It is thus important to ascertain how keeping ξ finite—as always the case in physical realizations—influences the physics at stake. The role of ξ in the large scale limit is exemplified specially in the context of functional renormalization group (FRG),[30,31] where at large scale the roughness arises from the zero-temperature fixed point of the renormalization flow hence displaying no temperature dependence—in contrast to pure scaling predictions (in other words, having ξ finite seems to influence temperature scaling exponents at large distance[29]).

In this paper, we address the issue of the role of ξ concerning the roughness scaling and the temperature regimes. We focus on the roughness of a one-dimensional static interface subjected to "random-bond" disorder, at finite temperature. It is known that at short lengthscale disorder plays no role and the interface is in a thermal regime ($\zeta_{\mathrm{th}}=\frac{1}{2}$) while at large lengthscale the interface is in the RM regime, characterized by a roughness exponent $\zeta_{\mathrm{RM}}=\frac{2}{3}$ (see Refs. 17, 22, and 23). We examine in detail the way the roughness crosses over from thermal to RM behavior, and, in particular, whether there is one or several crossover lengthscales, possibly allowing for a nontrivial "intermediate regime." We tackle these problems by using a Gaussian variational method (GVM).[32–35] Although this method is only approximate, it allows rather complete calculations for the roughness $B(r)$. The alternative methods are not so well suited to analyze this issue for a one-dimensional interface. Even though numerical methods such as Monte Carlo,[36] Langevin,[37] or transfer-matrix[38] methods are efficient to deal with the interface, one would need to implement them for very large system sizes, in order to tackle the issue of crossover lengthscales. As for the FRG approach,[30,31] it is based on an expansion in $\epsilon=4-d$ for a manifold of internal dimension d and may not be suited for our case of interest ($d=1$).

The plan of the paper is as follows. In Sec. II we introduce the DES description of a 1D interface. We show how the replica trick allows to make the average over disorder. In Sec. III we detail the variational procedure, originally introduced by Mézard and Parisi,[33] that we use in the paper to obtain an approximation of the various physical properties of the interface, and, in particular, the correlation function $B(r)$. The corresponding roughness is computed in Sec. IV, along with the crossover lengthscales separating its different power-law regimes, and their temperature dependence. In Sec. V we present a second GVM procedure, this time in direct-space representation, on a "toy model" which has been argued to be an effective model for the study of a directed polymer's end-point fluctuations, and on which the model of a 1D interface can carefully be mapped. In Sec. VI we examine how generic scaling arguments shed light on the interface and the toy-model results. The two GVM results are compared in Sec. VII, where consequences of our results for experiments on ferromagnetic domain walls are discussed altogether. We finally conclude in Sec. VIII. We present for reference standard Flory arguments in Appendix A and we recall in Appendix B some useful properties of hierarchical matrices.

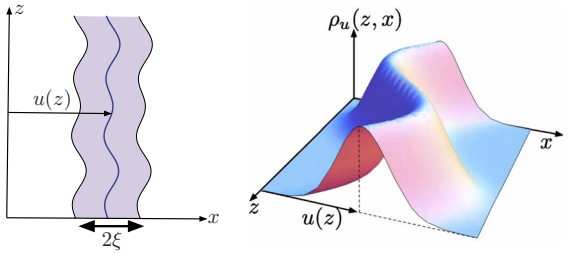

FIG. 1. (Color online) (Left) Displacement from a given flat configuration described by the z axis. (Right) Gaussian density $\rho_u(z,x)$ centered on the position $(z,u(z))$ of the interface.

II. MODEL OF A 1D INTERFACE

A. Model

In the DES framework, an interface can be described as an elastic manifold of dimension d with m transverse components, submitted to the random potential of a physical space of dimension $D=d+m$. The coordinates in this space can thus be split between the *internal* and *transverse* coordinates of the interface, respectively, $(z,x)\in\mathbb{R}^d\times\mathbb{R}^m=\mathbb{R}^D$. In the case $d=m=1$ (simply denoted "1+1" for DPs), a one-dimensional interface is thus described as an elastic line living in a bidimensional plane with a disordered energy landscape that will be defined below. Restricting ourselves to the case without bubbles nor overhangs, each configuration of the interface can be indexed by a univalued displacement field $u(z)$ which parametrizes the position $(z,u(z))$ of the interface along its internal direction z. This is schematically indicated in Fig. 1(a).

In disordered systems there is no strict spatial translational invariance but it can be recovered statistically once the disorder is averaged out. Thereafter, we will thus mostly work in Fourier-transform representation and denote the Fourier modes along z and x, respectively, q and λ. However there are in fact both infrared and ultraviolet cutoffs in those Fourier modes since a physical realization of an interface lives in a finite bidimensional plane of typical size L and is supported by a sublattice (e.g., a crystal in a solid) whose spacing $1/\Lambda$ defines the smallest physical lengthscale in the system. The cutoffs $1/L<q,\lambda<\Lambda$ will be conveniently reintroduced whenever needed to cure nonphysical divergences in Fourier-transform integrals. Thereafter we use the notation $\bar{d}^dq\equiv\frac{d^dq}{(2\pi)^d}$, as well as $\bar{\delta}^{(d)}(q)\equiv(2\pi)^d\delta^{(d)}(q)$, and similarly for other Fourier modes.

More importantly, in order to implement a finite interface width ξ into this model, we introduce the density of the interface $\rho_u(z,x)$ which is positive and normalized at fixed z by $\int_{\mathbb{R}}dx\cdot\rho_u(z,x)=1$, decreases significantly for $|x-u(z)|>\xi$ and tends to a Dirac δ function when $\xi\to0$. As schematized in

Fig. 1(b) we choose the simplest smooth density which is a Gaussian centered on $(z,u(z))$, of uniform standard deviation ξ, whose Fourier representation is thus

$$\rho_u(z,x) = \int_{\mathbb{R}} đ\lambda \cdot e^{i\lambda[x-u(z)]} e^{-\lambda^2\xi^2/2}. \quad (1)$$

The interface is subject to a random potential $V(z,x)$ whose distribution is Gaussian and uncorrelated in space. This corresponds to the limit of the collective pinning by many weak impurities. Denoting the statistical average over disorder by an overline, since it is Gaussian it is fully defined by

$$\overline{V(z,x)} = 0, \quad \overline{V(z,x)V(z',x')} = D \cdot \delta(z-z')\delta(x-x'), \quad (2)$$

where D is the strength of disorder.

We can now construct the DES Hamiltonian of the interface, which is the sum of the energetic cost of its distortions $\mathcal{H}_{\rm el}[u]$ and the contribution of the disordered energy landscape $\mathcal{H}_{\rm dis}(u,V]$. We assume that the elastic limit $|\nabla_z u(z)| \ll 1$ is realized and that the elasticity is short range so that the energy per Fourier mode $u_q \equiv \int_{\mathbb{R}} dz \cdot u(z) e^{iqz}$ is cq^2, where c is the elastic constant. The mode $u_{q=0}$ corresponds to the mean position of the interface, and introduces an additive constant in $\mathcal{H}_{\rm el}$ which will disappear in the Boltzmann weight and moreover does not contribute to the roughness. It can thus be put equal to zero directly in the elastic Hamiltonian by the *ad hoc* redefinition of u. We assume a random-bond disorder, i.e., that the interface couples locally to the random potential. Thus the full Hamiltonian $\mathcal{H}$ is given by

$$\mathcal{H}[u,V] = \mathcal{H}_{\rm el}[u] + \mathcal{H}_{\rm dis}[u,V], \quad (3)$$

$$\mathcal{H}_{\rm el}[u] = \frac{c}{2}\int_{\mathbb{R}} dz \cdot [\nabla_z u(z)]^2 = \frac{1}{2}\int_{\mathbb{R}} đq \cdot cq^2 u_{-q} u_q, \quad (4)$$

$$\mathcal{H}_{\rm dis}[u,V] = \int_{\mathbb{R}^2} dz dx \cdot \rho_u(z,x) V(z,x). \quad (5)$$

Note the alternative formulation of the $\mathcal{H}_{\rm dis}$ with an effective random potential $\tilde{V}$ coupled to a zero-width interface

$$\mathcal{H}_{\rm dis}[u,\tilde{V}] = \int_{\mathbb{R}} dz \cdot \tilde{V}(z,u(z)) \quad (6)$$

and its associated disorder distribution

$$\overline{\tilde{V}(z,x)} = 0, \quad \overline{\tilde{V}(z,x)\tilde{V}(z',x')} = \delta(z-z')R_\xi(x-x'), \quad (7)$$

where $R_\xi(u)$ is up to an additive constant the usual correlator of the disorder which is the key function renormalized in FRG procedures on DES.[31,34] It corresponds to the overlap between two densities ρ_u in our formulation and encodes the statistical translational invariance of the random potential. Note that $R_\xi(u_z,u'_z) \equiv D\int_{\mathbb{R}} dx \cdot \rho_u(z,x)\rho_{u'}(z,x)$ inherits both the translational invariance and the symmetry of the density. The Gaussian density in Eq. (1) translates into the following Gaussian correlator:

$$R_\xi(u-u') = D \cdot \int_{\mathbb{R}} đ\lambda \cdot e^{i\lambda(u-u')} e^{-\lambda^2\xi^2}. \quad (8)$$

So the parameter ξ can be seen either as the width of the interface or as the disorder correlation length (or a convolution of both). In previous GVM computations on DES (Refs. 33 and 34) the correlator $R(u)$ was assumed to exhibit an asymptotic power-law behavior whose exponent depended on the university class of the disorder. Here we focus on the role of a finite ξ rather than on this asymptotic behavior, following closely a similar approach of periodic DES.[32]

B. Statistical averages

The static properties of an interface are accessible by averaging over its thermal fluctuations and the stochastic variable V which is associated to each configuration of quenched disorder, so two statistical averages have to be successively performed for a given observable $\mathcal{O}$. The first one is the thermal average at fixed disorder $\langle\mathcal{O}\rangle_V$ using the Boltzmann weight $e^{-\beta\mathcal{H}[u,V]}/Z_V$, where $\beta=1/T$ is the inverse of the temperature (taking the Boltzmann constant $k_B=1$) and Z_V the canonical partition function

$$Z_V = \int \mathcal{D}u \cdot e^{-\beta\mathcal{H}[u,V]}, \quad (9)$$

$$\langle\mathcal{O}\rangle_V = \frac{1}{Z_V}\int \mathcal{D}u \cdot \mathcal{O}[u] \cdot e^{-\beta\mathcal{H}[u,V]}, \quad (10)$$

where the functional integral $\int\mathcal{D}u$ sums over all possible configurations u of the interface.

The second one is the average over disorder $\bar{\mathcal{O}}$ which has already been introduced in Eq. (2), assuming that the system is large enough to be disorder self-averaging (the equivalent of ergodicity for thermal averages).[35] To recover a translational invariance and be able to work in Fourier space, one would like to average technically first over disorder. This can in fact be done using the well-known replica trick.[35] Indeed, introducing n replicas of the partition function at fixed disorder Z_V, n being an arbitrary integer, we can replace $1/Z_V$ in the thermal average in Eq. (10) by $\lim_{n\to 0} Z_V^{n-1}$ under the (strong) assumption that at the end of our computations the analytical continuation $n\to 0$ is well defined and physically meaningful. This gives

$$\langle\mathcal{O}\rangle_V = \lim_{n\to 0}\int \mathcal{D}u_1(\cdots)\mathcal{D}u_n \cdot \mathcal{O}[u_1] \cdot e^{-\beta\Sigma_{a=1}^n \mathcal{H}[u_a,V]}. \quad (11)$$

Using the linearity in V of $\mathcal{H}_{\rm dis}$ in Eq. (5) and the Gaussian distribution of disorder in Eq. (2), we can then explicitly average over disorder and define an effective replicated Hamiltonian $\tilde{\mathcal{H}}$ which couples all the replicas $[\vec{u}\equiv(u_1,\ldots,u_n)]$

$$\overline{\langle \mathcal{O} \rangle} = \lim_{n \to 0} \int \mathcal{D}u_1(\cdots)\mathcal{D}u_n \cdot \mathcal{O}[u_1] \cdot \overline{e^{-\beta \sum_{a=1}^{n} \mathcal{H}[u_a, V]}}$$

$$\equiv \lim_{n \to 0} \int \mathcal{D}u_1(\cdots)\mathcal{D}u_n \cdot \mathcal{O}[u_1] \cdot e^{-\beta \tilde{\mathcal{H}}[\vec{u}]}, \tag{12}$$

where

$$\tilde{\mathcal{H}}[\vec{u}] = \sum_{a=1}^{n} \mathcal{H}_{\mathrm{el}}[u_a] - \frac{\beta}{2} \int_{\mathbb{R}} dz \cdot \sum_{a,b=1}^{n} R_{\xi}(u_a(z) - u_b(z)). \tag{13}$$

We have thus reformulated the problem of one interface in a random potential V into a system of n coupled interfaces without disorder, in the limit $n \to 0$.

Finally, using Eqs. (4) and (8), we explicit the effective replicated Hamiltonian which is exact up to this point, diagonal in Fourier space due to translational invariance and depends only on the parameters $\{\xi, c, D, T\}$

$$\tilde{\mathcal{H}}[\vec{u}] = \tilde{\mathcal{H}}_{\mathrm{el}}[\vec{u}] + \tilde{\mathcal{H}}_{\mathrm{dis}}[\vec{u}],$$

$$\tilde{\mathcal{H}}_{\mathrm{el}}[\vec{u}] = \frac{1}{2} \int_{\mathbb{R}} đq \cdot cq^2 \sum_{a=1}^{n} u_a(-q) u_a(q),$$

$$\tilde{\mathcal{H}}_{\mathrm{dis}}[\vec{u}] = -\frac{\beta D}{2} \int_{\mathbb{R}} đ\lambda \cdot e^{-\lambda^2 \xi^2} \int_{\mathbb{R}} dz \cdot \sum_{a,b=1}^{n} e^{i\lambda[u_a(z) - u_b(z)]}. \tag{14}$$

C. Roughness and displacement correlation function

In order to study the static fluctuations of the position of the interface, we compute the variance of the relative displacements of two points of the interface: $B(z_1, z_2) \equiv \overline{\langle [u(z_1) - u(z_2)]^2 \rangle}$. The disorder average leads back to translational invariance $B(z_1, z_2) = B(z_1 - z_2, 0)$. One can thus define the roughness as a function of the lengthscale r, formally the two-point correlation function of our system

$$B(r) \equiv \overline{\langle [u(r) - u(0)]^2 \rangle}, \tag{15}$$

which is the Fourier transform of the structure factor $S(q)$

$$S(q) \equiv \int đ\tilde{q} \cdot \overline{\langle u_{-\tilde{q}} u_q \rangle},$$

$$B(r) = \int đq \cdot 2[1 - \cos(qr)] S(q). \tag{16}$$

If the DES displays a scale invariance in its fluctuations, the roughness is expected to follow a power-law behavior $B(r) \sim r^{2\zeta}$, with a corresponding *roughness exponent* ζ. To describe the possible interplay between different terms in $B(r)$ we generalize the definition of ζ

$$\zeta(r) \equiv \frac{1}{2} \frac{\partial \log B(r)}{\partial \log r} \tag{17}$$

whose different values characterize the different regimes of fluctuations depending on the lengthscale considered. Along with the r-independent prefactor of $B(r)$ it probes the physics at different lengthscales and a roughness regime is actually defined by a constant value of ζ.

If the exact replicated Hamiltonian could be put into a quadratic replicated form, diagonal in Fourier space, such as

$$\mathcal{H}_0[\vec{u}] = \frac{1}{2} \int đq \sum_{a,b=1}^{n} u_a(-q) G_{ab}^{-1}(q) u_b(q) \tag{18}$$

then the corresponding structure factor would be

$$S_0(q) = \beta^{-1} \cdot \lim_{n \to 0} G_{aa}(q). \tag{19}$$

In the absence of disorder ($\mathcal{H} = \mathcal{H}_{\mathrm{el}}$) the replicas are uncoupled and $G_{ab}^{-1}(q) = cq^2 \cdot \delta_{ab}$, so the structure factor is proportional to the "thermal propagator" $\frac{1}{cq^2}$ which leads to the purely thermal roughness of a 1D interface $B_{\mathrm{th}}(r) = \frac{Tr}{c}$. The exact Hamiltonian (14) is diagonal in Fourier space, but it cannot be put into a quadratic form because of the coupling of all replicas $\Sigma_{a,b=1}^{n} e^{i\lambda[u_a(z) - u_b(z)]}$. This forbids the direct use of Eq. (19) for the computation of $S(q)$. To be able to do so, we thus approximate $\tilde{\mathcal{H}}$ in the Boltzmann weight in Eq. (12) by a quadratic replicated Hamiltonian $\mathcal{H}_0$ optimized by GVM, as explained in the next section.

III. GVM AND FULL-RSB ANSATZ

The GVM has already been applied to DES, periodic systems[32] as well as manifolds,[33,34] to study the temperature dependence of observables at thermodynamic equilibrium. Here we extend these computations specifically to the case of a one-dimensional interface of finite width ξ, in order to explore its small-lengthscales behavior.

We follow in this derivation the main steps outlined in Ref. 32 for periodic systems. One important difference comes from the fact that in our case the variable λ in Eq. (14) is continuous while it takes discrete values for periodic systems. As we will see this has drastic consequence for the physical properties of the system as well as for the calculation itself.

A. GVM in Fourier representation

The variational method consists in replacing, in the Boltzmann weight of statistical averages, the exact Hamiltonian $\tilde{\mathcal{H}}$ or more generally the exact action of a system by a trial Hamiltonian $\mathcal{H}_0$ with variational parameters. The criterion chosen to optimize this approximation is given by the Gibbs-Bogoliubov inequality, which states that the free energy $\mathcal{F}$ of a system is minimum at equilibrium, i.e., when the probability measure of the system is precisely described by its exact Boltzmann weight

$$\mathcal{F} \leq \mathcal{F}_{\mathrm{var}} \equiv \mathcal{F}_0 + \langle \tilde{\mathcal{H}} - \mathcal{H}_0 \rangle_0, \tag{20}$$

where $\mathcal{F}_{\mathrm{var}}$ is the variational free energy associated to the trial Hamiltonian $\mathcal{H}_0$ and which has to be minimized, $\mathcal{F}$ and $\mathcal{F}_0$ the free energies corresponding, respectively, to $\tilde{\mathcal{H}}$ and $\mathcal{H}_0$ (they are defined with respect to their corresponding par-

tition function $Z \equiv e^{-\beta \mathcal{F}}$), and $\langle \mathcal{O} \rangle_0$ the statistical average defined over $\mathcal{H}_0$.

For the replicated Hamiltonian (14), the trial Hamiltonian $\mathcal{H}_0$ is chosen quadratic of the generic form in Eq. (18), parametrized[33] by a $n \times n$ matrix $G_{ab}^{-1}(q)$. Its inverse matrix gives thus directly access to the correlation functions

$$\langle u_a(-\tilde{q}) u_b(q) \rangle_0 = \beta^{-1} \cdot G_{ab}(q) \cdot \delta(\tilde{q} - q) \tag{21}$$

and in particular to the structure factor $S(q)$ and the roughness $B(r)$ itself. The minimization of $\mathcal{F}_{\rm var}$ with respect to the variational parameters $G_{ab}(q)$ (the Green's function of $\mathcal{H}_0$) gives a saddle point equation for the optimal matrix $G_{ab}^{-1}(q)$. Besides, the replica trick constrains the structure of G_{ab}^{-1}, which must be a *hierarchical* matrix. In Appendix B we recall some useful properties of such matrices, including their inversion formulas in the limit $n \to 0$ which will be used extensively thereafter.

The extremalization condition $\partial \mathcal{F}_{\rm var} / \partial G_{ab}(q) = 0$ can be reformulated as

$$G_{ab}^{-1}(q) = cq^2 \cdot \delta_{ab} - \sigma_{ab},$$

$$\sigma_{ab} \equiv -\beta \frac{\partial}{\partial G_{ab}(q)} \langle \tilde{\mathcal{H}}_{\rm dis} \rangle_0. \tag{22}$$

Note that σ_{ab} is independent of the Fourier mode q since $\tilde{\mathcal{H}}_{\rm dis}$ is itself purely local in z.

We point out that although the GVM approach is only approximate in our context, it becomes exact[34] in the limit of an infinite number of transverse components $m \to \infty$. The extremalization equations then appear as genuine saddle-point equations with $1/m$ playing the role of a small parameter. By extension we extensively use thereafter this improper denomination to refer to Eq. (22). Furthermore, one could for completeness check the stability of the GVM solution by considering its associated Hessian matrix.[33] This problem can be quite complicated so we simply check the physical consistency of our results in what follows.

B. Saddle point equation in the full-RSB formulation

To compute explicitly σ_{ab} in Eq. (22) we start from Eq. (14) and performing the Gaussian statistical average

$$\langle e^{i\lambda [u_a(z) - u_b(z)]} \rangle_0 = e^{-\lambda^2 \langle [u_a(z) - u_b(z)]^2 \rangle_0 / 2} \tag{23}$$

we have

$$\langle \tilde{\mathcal{H}}_{\rm dis} \rangle_0 = -\frac{\beta D}{2} \int_{\mathbb{R}} dz \int_{\mathbb{R}} \text{đ}\lambda \cdot \sum_{a,b=1}^{n} e^{-\lambda^2 \{ \xi^2 + \langle [u_a(z) - u_b(z)]^2 \rangle_0 / 2 \}}, \tag{24}$$

where the variance of the relative displacement between two replicas at fixed z is obtained by applying Eq. (21) on its Fourier-transform representation. This gives the translational-invariant quantity:

$$\langle [u_a(z) - u_b(z)]^2 \rangle_0 = T \int_{\mathbb{R}} \text{đ}q [G_{aa}(q) + G_{bb}(q) - 2G_{ab}(q)]. \tag{25}$$

Performing $\partial / \partial G_{ab}(q)$ and denoting $G_{aa} \equiv \tilde{G}$ we eventually obtain σ_{ab}, separating off-diagonal $a \neq b$ terms

$$\sigma_{a \neq b} = \frac{D}{T} \int_{\mathbb{R}} \text{đ}\lambda \cdot \lambda^2 \cdot e^{-\lambda^2 \{ \xi^2 + T \int \text{đ}q [\tilde{G}(q) - G_{a \neq b}(q)] \}} \tag{26}$$

from the diagonal $a = b$

$$\sigma_{aa} = -\sum_{a' \neq a} \sigma_{a' \neq a} \equiv \tilde{\sigma}. \tag{27}$$

Note that $\langle \tilde{\mathcal{H}}_{\rm dis} \rangle_0$ is extensive in the interface size [see Eq. (24)] whereas σ_{ab} is intensive as expected since $\int dz$ has disappeared.

We can compute the connected part of the hierarchical matrix $\hat{G}^{-1}(q)$

$$G_c^{-1}(q) \equiv \sum_{a'} G_{aa'}^{-1}(q) = cq^2 - \tilde{\sigma} - \sum_{a'} \sigma_{a' \neq a} = cq^2. \tag{28}$$

Using Eq. (B3) we know that

$$G_c(q) = \frac{1}{cq^2}. \tag{29}$$

In this GVM framework the connected part of the hierarchical matrices $\hat{G}^{-1}(q)$ and $\hat{G}(q)$ have thus a straightforward physical meaning: in the Hamiltonian it represents the elastic energy per Fourier mode $G_c^{-1}(q) = cq^2$ and in the Green's function it gives back the thermal propagator $G_c(q) = \frac{1}{cq^2}$. On one hand the irruption of disorder populates by construction the off-diagonal elements of $\hat{G}^{-1}(q)$ with the q-independent coupling terms $-\sigma_{a \neq b}$ under the constraint in Eq. (28). On the other hand the invariance of $G_c(q)$ is a consequence of the statistical tilt symmetry of the DES description.[31,32,39–41]

To determine the actual propagators we consider the generic case of a full replica-symmetry breaking (RSB) Ansatz, the off-diagonal term being parametrized by $u \in [0,1]$

$$\hat{G}^{-1}(q) \equiv (G_c^{-1}(q) - \tilde{\sigma}, -\sigma(u)) \Leftrightarrow \hat{G}(q) \equiv (\tilde{G}(q), G(q,u)), \tag{30}$$

where the definition of the connected part G_c^{-1} is consistent with the continuous version in Eq. (B8) for the definition of $\tilde{\sigma}$ in Eq. (27). The saddle point Eq. (26) becomes

$$\sigma(u) = \frac{D}{T} \int_{\mathbb{R}} \text{đ}\lambda \cdot \lambda^2 \cdot e^{-\lambda^2 \{ \xi^2 + T \int \text{đ}q [\tilde{G}(q) - G(q,u)] \}}, \tag{31}$$

$$= \frac{D}{4\pi T} \left\{ \xi^2 + T \int_{\mathbb{R}} \text{đ}q [\tilde{G}(q) - G(q,u)] \right\}^{-3/2} \tag{32}$$

and the relation between $[\tilde{G}(q) - G(q,u)]$ and $\sigma(u)$ can be made explicit using the inversion formulas (B11) and (B12) and the definition in Eq. (B9) of the self-energy $[\sigma](u)$ which appears in them. $\sigma(u)$ must thus satisfy this self-consistent

saddle-point equation but we will work alternatively with $\sigma(0)$ and $[\sigma](u)$.

C. Determination of $\sigma(u)$ and $[\sigma](u)$

We assume that $\sigma(u)$ is continuous by sector and aim to point out its power-law behavior using the following implication of the definition in Eq. (B9):

$$[\sigma]'(u) = u \cdot \sigma'(u). \tag{33}$$

We first apply ∂_u on Eq. (32), then identify a power of $\sigma(u)$ and use Eqs. (B12) and (B15) to make explicit the following term:

$$\begin{aligned}
&\partial_u \left\{ T \int_{\mathbb{R}} đq [\tilde{G}(q) - G(q,u)] \right\} \\
&= T \int_{\mathbb{R}} đq \cdot \partial_u \left\{ \int_u^1 \frac{\sigma'(v)}{[cq^2 + [\sigma](v)]^2} \right\} \\
&= -T \int_{\mathbb{R}} đq \frac{\sigma'(u)}{[cq^2 + [\sigma](u)]^2} \\
&= -\frac{T}{4\sqrt{c}} \cdot \sigma'(u) \cdot [\sigma](u)^{-3/2}.
\end{aligned} \tag{34}$$

We thus obtain the new equation

$$\sigma'(u) = \sigma'(u) \cdot (T\sigma(u))^{5/3} [\sigma](u)^{-3/2} \frac{3\pi^{1/3}}{2^{5/3} D^{2/3} c^{1/2}}. \tag{35}$$

We have either $\sigma'(u)=0$ which corresponds to plateaux in $\sigma(u)$ and possibly to a full replica-symmetric (RS) solution or if $\sigma'(u) \neq 0$ we have a strictly monotonous segment that should satisfy the new equation

$$T\sigma(u) = [\sigma](u)^{9/10} 2 \left(\frac{D^4 c^3}{3^6 \pi^2} \right)^{1/10}. \tag{36}$$

Note that by definition of the self-energy in Eq. (B9) we have $[\sigma](0)=0$ so the relation (36) implies in particular that $\sigma(0)=0$, property that can be checked *a posteriori* by plugging our full-RSB solution directly into the initial saddle point Eq. (32).

Differentiating again Eq. (36) and using Eq. (33) to reintroduce a u dependence, we finally obtain for the monotonous segments of the self-energy $[\sigma](u)$

$$[\sigma](u) = \frac{3^{14}}{5^{10}\pi^2} c^3 D^4 (u/T)^{10} \equiv A_{(c,D)} (u/T)^{10}. \tag{37}$$

It is important to note that the power-law form $(u/T)^\nu$, which will actually condition the asymptotic temperature dependence of the roughness, is totally constrained by the GVM procedure. Indeed, we can track down the temperature factors in the previous procedure: the extremalization condition of $\mathcal{F}_{\text{var}}$ introduces a first β in Eq. (22) via $\partial \mathcal{F}_0 / \partial G_{ab}(q) = \beta^{-1} G_{ab}^{-1}(q)$. The derivative involving $\langle \tilde{\mathcal{H}}_{\text{dis}} \rangle_0$ introduces no new T dependence because its overall β factor is canceled through the derivative $\partial / \partial G_{ab}(q)$ of its exponential argument. The only T factor which remains in the relation (36) between $\sigma(u)$ and $[\sigma](u)$ eventually leads to the $(u/T)^\nu$ dependence once the u dependence is made explicit. We will go back to that property in Sec. IV E and compare its implications for the asymptotic T dependence of the roughness for the 1D interface versus the prediction of another model in Sec. VII.

We have obtained so far that for the values of u for which $\sigma(u)$ is not constant, it must obey

$$\sigma(u) = \frac{10}{9} \frac{A_{(c,D)}}{T} (u/T)^9 + \text{cte}, \tag{38}$$

where this last constant has to be determined in relation to the possible plateaux and cutoffs imposed on the Ansatz $\sigma(u)$, using the saddle point Eq. (32) to fix them.

In addition to the above power-law behavior we must consider the possibility of a plateau in $\sigma(u)$. One such trivial example would be a totally RS solution for which $\sigma(u)$ is independent of u. In that case, in the saddle-point Eq. (31) the term $\tilde{G}(q) - G(q,u) = G_c(q) = \frac{1}{cq^2}$ as explained in Eq. (B5) and thus

$$\sigma_{\text{RS}}(u) = \sigma_{\text{RS}}(0) = \frac{D}{T} \int_{\mathbb{R}} đ\lambda \cdot \lambda^2 \cdot e^{-\lambda^2 \xi^2} e^{-\lambda^2 \int_{\mathbb{R}} đq \cdot G_c(q)} = 0. \tag{39}$$

The RS solution completely eliminates all effects of disorder, it is thus clearly unphysical, as was the case in the higher dimensional cases[33] and the periodic ones.[32]

To take into account the possible presence of plateaux we thus look for a full-RSB solution $\sigma(u)$ with a single cutoff $v_c \in (0,1)$ of the form

$$\begin{aligned}
\sigma(u \leq v_c) &= \frac{10}{9} \frac{A_{(c,D)}}{T} (u/T)^9 + \sigma(0), \\
\sigma(u \geq v_c) &= \sigma(v_c)
\end{aligned} \tag{40}$$

and for the self-energy

$$\begin{aligned}
[\sigma](u \leq v_c) &= A_{(c,D)} (u/T)^{10}, \\
[\sigma](u \geq v_c) &= [\sigma](v_c), \\
A_{(c,D)} &\equiv \frac{3^{14}}{5^{10}\pi^2} c^3 D^4.
\end{aligned} \tag{41}$$

Up to this point the width ξ does not appear in these expressions. It is in fact encoded into the single full-RSB cutoff $v_c(\xi)$. The equation for this cutoff is obtained by checking the consistency of the solution (41) with the initial saddle point Eq. (32). Using the inversion formula (B12) adapted to the presence of a cutoff $\sigma'(u \geq v_c)=0$, then integrating over the q modes with Eqs. (B14) and (B15), and inserting our full-RSB solution in Eq. (41) we have

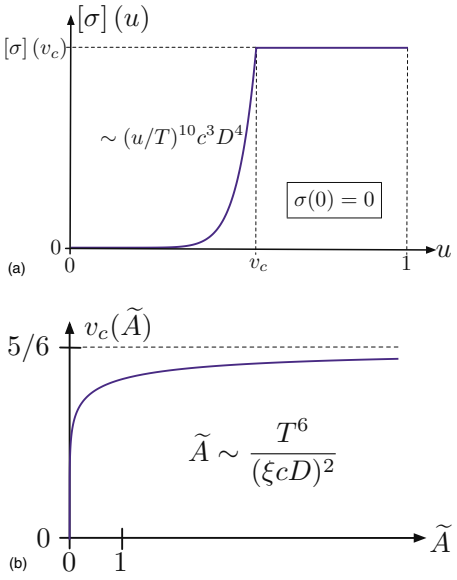

FIG. 2. (Color online) GVM solution for the 1D interface. (a) Self-energy $[\sigma](u)$ given by Eq. (41); using $[\sigma]'(u)=u\sigma'(u)$ and $\sigma(0)=0$ the expression (40) for $\sigma(u)$ can be recovered. (b) Full-RSB cutoff v_c as a function of $\tilde{A} \sim \frac{T^6}{(\xi c D)^2}$, obtained by solving the polynomial Eq. (45). It starts linearly at $\tilde{A} \to 0$ and saturates to 5/6 at $\tilde{A} \to \infty$, yielding in particular the low-temperature dependence given by Eq. (46).

$$T\int_{\mathbb{R}} dq \cdot [\tilde{G}(q) - G(q,u)]$$
$$= T\frac{[\sigma](v_c)^{-1/2}}{2\sqrt{c}} + T\int_u^{v_c} dv \cdot \sigma'(v) \cdot \frac{[\sigma](v)^{-3/2}}{4\sqrt{c}}$$
$$= \frac{5^5}{2\times 3^7}\pi\frac{1}{(cD)^2}\left[\left(\frac{v_c}{T}\right)^{-6}(v_c - 5/6) + \frac{5}{6}\left(\frac{u}{T}\right)^{-6}\right]. \quad (42)$$

Substituting this expression into Eq. (32), the full-RSB Ansatz $\sigma(u \le v_c)$ in Eq. (40) is self-consistent if the ξ dependence cancels the v_c terms

$$\xi^2 + \frac{5^5}{2\times 3^7}\pi\frac{1}{(cD)^2}\left(\frac{v_c}{T}\right)^{-6}(v_c - 5/6) = 0 \quad (43)$$

and also if $\sigma(0)=0$. This last condition is enforced by Eq. (36) and can be checked *a posteriori* by combining Eqs. (32), (42), and (43)

$$\sigma(0) = \frac{D}{T}\int_{\mathbb{R}} d\lambda \cdot \lambda^2 \cdot \lim_{u\to 0} \exp\left[-\lambda^2 \frac{5^5}{2\times 3^7}\pi\frac{T^6}{(cD)^2}\cdot u^{-6}\right] = 0. \quad (44)$$

The single full-RSB cutoff is thus given by the polynomial equation

$$v_c^6 = \tilde{A}(5/6 - v_c), \quad \tilde{A} \equiv \frac{5^5}{2\times 3^7}\pi\frac{T^6}{(\xi c D)^2} \quad (45)$$

whose solution is plotted in Fig. 2(b). The factor 5/6 can be shown to be closely related to the Flory exponent ζ_F in $d=1$ (cf. Appendix A); the presence of a cutoff $v_c < 5/6 = (2\zeta_F|_{d=m=1})^{-1}$ in the full-RSB Ansatz $[\sigma](u)$ is in fact necessary for $[\sigma](u)$ to be a solution of the GVM saddle point equation. All the above results are summarized in Fig. 2.

D. Low versus high-temperature limits of $[\sigma](u)$

Before computing the roughness $B(r)$, which we will do in the next section, we have to explicit the low- and the high-temperature limits of this solution since we also aim to probe the T dependence of the roughness. An explicit analytical expression for $v_c \in (0,5/6)$ can be obtained for the two opposite limits of $\tilde{A}$, which at fixed $\xi, D > 0$ correspond respectively to $T \to 0$ and $T \to \infty$ and yield the following asymptotic behavior:

$$v_c \overset{\tilde{A}\to 0}{\approx} \frac{5}{6}\left(\frac{4}{3}\sqrt{\pi}\right)^{1/3}\frac{T}{(\xi c D)^{1/3}} \to 0, \quad (46)$$

$$v_c \overset{\tilde{A}\to \infty}{\approx} 5/6 + 0^-. \quad (47)$$

The crossover between the two regimes of high and low temperature is in fact conditioned by the value of the dimensionless parameter $\tilde{A}$ in the equation for $v_c(\xi)$ (45); an arbitrary definition of a characteristic temperature is naturally given by the crossover between the two opposite limits $\tilde{A} \to \infty$ and $\tilde{A} \to 0$, which happens at

$$\tilde{A} = 1 \Leftrightarrow \frac{T_c}{(\xi c D)^{1/3}} = \left(\frac{2\times 3^7}{5^5\pi}\right)^{1/6} \approx 0.87 \quad (48)$$

and this last constant is of order 1. Note that this characteristic temperature depends explicitly on the width ξ, in such a way that the limits $T \to 0$ and $\xi \to 0$ cannot be exchanged with impunity: imposing $\xi=0$ from the beginning is equivalent to considering exclusively the "high–temperature" regime, and the somehow nonphysical regime at simultaneously zero temperature and zero width has to be carefully handled.

The first limit in Eq. (46) implies that when the thermal fluctuations are suppressed, $[\sigma](u)$ tends to a nonzero RS solution, since $v_c \to 0$ and

$$[\sigma](v_c) \overset{\tilde{A}\to 0}{\approx} \frac{1}{4}\left(\frac{3}{4\sqrt{\pi}}\right)^{2/3} \cdot \xi^{-10/3} c^{-1/3} D^{2/3}. \quad (49)$$

Increasing the strength of disorder D is compatible with this limit and indeed the self-energy is intuitively expected to increase with D.

On the contrary the decrease in D or ξ leads to the second limit in Eq. (47), in which the ξ dependence has been washed out from the GVM solution by the relatively large thermal fluctuations

$$[\sigma](v_c) \overset{\tilde{A}\to \infty}{\approx} \frac{3^4}{2^{10}\pi}\frac{c^3 D^4}{T^{10}}. \quad (50)$$

IV. GVM ROUGHNESS AND CROSSOVER LENGTHSCALES OF THE 1D INTERFACE

Using the definition of the structure factor in Eq. (16) in relation with the Green function of a quadratic Hamiltonian (19), we can now compute the corresponding roughness as a function of the lengthscale r along the internal coordinate z of the interface

$$B(r) = T\int_{\mathbb{R}} đq \cdot 2[1-\cos(qr)]\lim_{n\to 0}\widetilde{G}(q). \tag{51}$$

The inversion formula for $\lim_{n\to 0}\widetilde{G}(q)$ in Eq. (B10) contains two contributions [since $\sigma(0)=0$] which yield respectively a purely thermal and a disorder-induced roughness

$$B(r) = B_{\rm th}(r) + B_{\rm dis}(r), \tag{52}$$

$$B_{\rm th}(r) = T\int_{\mathbb{R}} đq \frac{2[1-\cos(qr)]}{cq^2} = \frac{Tr}{c}, \tag{53}$$

$$B_{\rm dis}(r) = T\int_{\mathbb{R}} đq \frac{2[1-\cos(qr)]}{cq^2}\int_0^1 \frac{dv}{v^2}\frac{[\sigma](v)}{cq^2+[\sigma](v)}. \tag{54}$$

The structure factor in $B_{\rm dis}(r)$ is a combination of propagators $\frac{(cq^2/[\sigma](v)+1)^{-1}}{cq^2}$ organized by the RSB parameter v, with an increasing self-energy $[\sigma](v)$ bounded by its value at the full-RSB cutoff $[\sigma](v_c)$. The corresponding roughness is eventually computed by integrating explicitly over the Fourier modes q.

A. GVM roughness of a 1D interface

Using the identity (B16) we obtain an analytical expression for a generic $[\sigma](v)$

$$B_{\rm dis}(r) = T\int_0^1 \frac{dv}{v^2}\cdot[\sigma](v)\cdot\int_{\mathbb{R}} đq \frac{2[1-\cos(qr)]}{cq^2[cq^2+[\sigma](v)]}$$
$$= \frac{T}{\sqrt{c}}\sum_{k=2}^{\infty}\frac{(-r/\sqrt{c})^k}{k!}\int_0^1 \frac{dv}{v^2}\cdot[\sigma](v)^{(k-1)/2}, \tag{55}$$

which simplifies for our full-RSB solution (41) into

$$B_{\rm dis}(r) = \frac{Tr_0}{c}\cdot v_c^{-1}\sum_{k=2}^{\infty}\frac{(r/r_0)^k}{k!}\left[\frac{1}{5k-6}+(1-v_c)\right], \tag{56}$$

where r_0 is a characteristic lengthscale which appears naturally in the formalism in order to obtain dimensionless quantities. It is defined by

$$[\sigma](v_c) \equiv cq_0^2 \overset{q_0\equiv 1/r_0}{\Leftrightarrow} r_0 = \sqrt{c/[\sigma](v_c)} \tag{57}$$

and can be made explicit using Eq. (41)

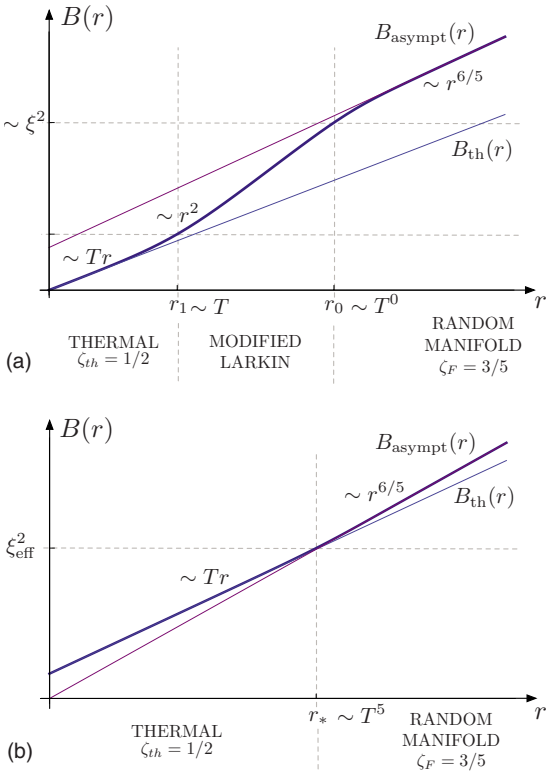

FIG. 3. (Color online) GVM prediction for the 1D-interface static roughness $B(r)$, in log-log representations; the slope of the curves corresponds to $2\zeta(r)$ as defined by Eq. (17) ($\xi=c=D=1$). (a) At low temperature ($T=10^{-3}$) an intermediate regime appears between the small and large lengthscales regimes, while (b) at high temperature ($T=10$) no intermediate regime occurs. The scalings of the different quantities, including crossover lengthscales, are recalled directly on the figures.

$$r_0 = \frac{5^5\pi}{3^7}\frac{1}{cD^2}\left(\frac{T}{v_c}\right)^5 \tag{58}$$

$B_{\rm dis}(r)$ is thus composed on one hand of the prefactor $\frac{Tr_0}{c}$ which fixes its dimensions and is actually the thermal roughness at the scale r_0, and on the other hand of a dimensionless series in (r/r_0) including the parameter v_c given by Eq. (45).

The whole displacement correlation function $B(r)$ is plotted in Fig. 3 where we distinguish the low versus high-temperature cases. In Fig. 4 we show the evolution of the roughness at increasing T and fixed D versus the other way around. A summary of the different roughness regimes along with their corresponding exponent ζ and their crossover lengthscales is given by Fig. 8(a).

1. At small lengthscales: Thermal regime

At small lengthscales the linear term of $B_{\rm th}(r)$ dominates the whole roughness and the 1D interface fluctuates as expected as if there were no disorder

$$B(r) \overset{r\to 0}{\approx} B_{\rm th}(r) = \frac{Tr}{c} \sim r^{2\zeta_{\rm th}}. \tag{59}$$

This defines the thermal regime of the roughness, of corresponding thermal exponent $\zeta_{\rm th}=1/2$.

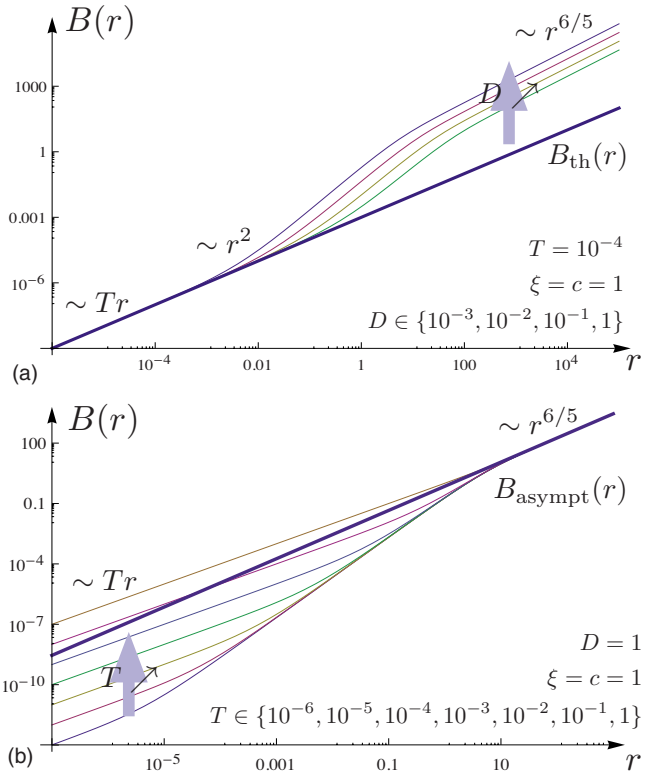

FIG. 4. (Color online) Evolution of the 1D-interface static roughness at finite width ξ. (a) At fixed T (low-temperature regime) all the roughness curves start from the same $B_{\rm th}(r)=\frac{Tr}{c}$ at small lengthscales, and behave asymptotically in $r^{6/5}$ with a T-independent prefactor increasing with disorder. (b) At fixed D all the roughness curves collapse on the same $B_{\rm asympt}(r)\sim T^0 r^{6/5}$ at large lengthscales [see Eq. (62)] and start from a microscopic thermal roughness which is boosted by increasing thermal fluctuations.

2. At large lengthscales: Random Manifold regime

To make explicit the asymptotic behavior at large lengthscales, we can reformulate the truncated alternated series in Eq. (56) using the following definition of the Euler Γ function and its generalization

$$\Gamma(a)=\int_0^\infty dt\, t^{a-1}e^{-t},$$

$$\Gamma(a,z)=\int_z^\infty dt\, t^{a-1}e^{-t}, \tag{60}$$

which yield

$$B_{\rm dis}(r)=\frac{Tr_0}{c}v_c^{-1}\Bigg\{(1-v_c)(e^{-r/r_0}-r/r_0-1)-r/r_0+\frac{1}{6}+(r/r_0)^{6/5}\left[-\frac{1}{6}\Gamma\left(-\frac{1}{5}\right)-\frac{1}{5}\Gamma\left(-\frac{6}{5},r/r_0\right)\right]\Bigg\}. \tag{61}$$

Since $\Gamma(-6/5,a)$ tends exponentially fast to 0 for increasing a, at large lengthscales the total roughness is dominated by the following power-law behavior

$$B(r)\overset{r\to\infty}{\approx}B_{\rm asympt}\equiv\frac{Tr_0}{c}v_c^{-1}\left(\frac{r}{r_0}\right)^{6/5}\sim r^{2\zeta_F} \tag{62}$$

with an overall numerical factor $[-\frac{1}{6}\Gamma(-\frac{1}{5})]\approx 0.970191$ and the Flory roughness exponent $\zeta_F=\frac{4-d}{4+m}\big|_{d=m=1}=3/5$ (see Appendix A). This asymptotic exponent which is not the exact one $\zeta_{\rm RM}=2/3$, is a consequence of the variational approximation. It leads in particular to an asymptotic *temperature independence* when r_0 is made explicit using Eq. (58)

$$B_{\rm asympt}=\frac{3}{5}\left(\frac{9}{\pi}\right)^{1/5}c^{-4/5}D^{2/5}r^{6/5}. \tag{63}$$

We will examine this point in more details in Sec. IV E.

B. Larkin length, RSB, and effective width

The RS section $u\geq v_c$ corresponds to small lengthscales (large q) in which the interface fluctuates purely thermally, whereas the full-RSB section $u\leq v_c$ corresponds to large lengthscales (small q) and encodes the disorder-induced metastability experienced by the interface in the RM regime. So the cutoff v_c, and consequently r_0 must correspond to the definition of a characteristic crossover lengthscale between two roughness regimes, namely, the Larkin length,[42] which marks the beginning of the RM regime.

Using the low- and high-temperature limits of $[\sigma](v_c)$, respectively, Eqs. (49) and (50), analytical expressions of the characteristic lengthscale r_0 are accessible at finite c and ξ

$$r_0\overset{T\to 0}{\approx}2\left(\frac{4\sqrt{\pi}}{3}\right)^{1/3}\cdot\xi^{5/3}c^{2/3}D^{-1/3}, \tag{64}$$

$$r_0\overset{T\to\infty}{\approx}\frac{2^5\pi}{3^2}\frac{T^5}{cD^2}. \tag{65}$$

At low temperatures it is temperature independent and depends explicitly on the width ξ, whereas at high temperature it is the opposite, and the microscopic parameter ξ is completely washed out. This leads in particular to a radical simplification of the prefactor $\frac{Tr_0}{c}v_c^{-1}$ in $B_{\rm dis}(r)$ at low temperature

$$B_{\rm dis}(r)\overset{T\to 0}{\approx}\frac{12}{5}\xi^2\sum_{k=2}^{\infty}\frac{(-r/r_0)^k}{k!}\left(\frac{1}{5k-6}+1\right), \tag{66}$$

which gives at $r=r_0$

$$B_{\rm dis}(r_0)\overset{T\to 0}{\approx}\frac{6}{5}\xi^2. \tag{67}$$

It follows from this last expression that r_0 satisfies the usual definition of the Larkin length L_c, i.e., the lengthscale at which the mean displacement of the interface is of the order of its width

$$u(L_c)\sim\sqrt{B(L_c)}\sim\xi. \tag{68}$$

At higher temperatures, if we want to keep r_0 as the Larkin length, i.e., associate the beginning of the RM regime and the breaking of the replica symmetry by imposing $r_0\equiv L_c$, we

have then to define an effective width ξ_{eff} with respect to the roughness at $r=r_0$

$$B_{\text{dis}}(r_0) \overset{T\to\infty}{\approx} \frac{Tr_0}{c}\frac{1}{5} \equiv \xi_{\text{eff}}^2, \tag{69}$$

$$\xi_{\text{eff}} = \frac{3}{2}\frac{T^3}{cD} \tag{70}$$

so at high temperature the interface "thickens" due to the increasing interplay of thermal fluctuations with disorder.

C. Crossover at low temperature: Modified Larkin regime

The end of the thermal regime can be defined as the lengthscale at which the quadratic term $\sim r^2$ in the sum of power-law corrections of $B_{\text{dis}}(r)$ becomes of the same order as the linear term of the thermal roughness

$$r_1 = r_0 \frac{2v_c}{5/4 - v_c}. \tag{71}$$

Note that r_1 does never diverge since $v_c < 5/6 < 5/4$. At low temperature it can be made explicit using Eq. (64)

$$r_1 \overset{T\to 0}{\approx} \frac{16}{9}(6\pi)^{1/3} T \cdot \xi^{4/3} c^{1/3} D^{-2/3}. \tag{72}$$

This increases linearly with the temperature and at some point will even merge with r_0, defining an upper characteristic temperature with the help of Eq. (45)

$$r_1 = r_0 \Leftrightarrow v_c = \frac{5}{12} \Leftrightarrow \frac{T_c}{(\xi c D)^{1/3}} = \left(\frac{3^2}{2^9\pi}\right)^{1/6} \approx 0.42. \tag{73}$$

Up to a factor 1/2 this criterion is equivalent to Eq. (48).

For intermediate lengthscales between r_1 and r_0 the roughness function shows a smooth connection between the thermal regime at $r<r_1$ and the RM regime at $r>r_0$, as can be seen in the low temperature case in Fig. 3(a). At fixed strength of disorder D and increasing T the crossovers r_1 and r_0 are getting closer and squeeze this intermediate regime, as can be seen in Fig. 4(b). In other dimensionalities this intermediate regime would be described by the Larkin model,[42] which predicts a power-law behavior of exponent $\zeta_L = \frac{4-d}{2}$. For the 1D interface ($d=m=1$) the perturbative expansion of the Larkin model is not valid, and this regime is described by a sum of power-law corrections in r, starting from the quadratic term $\sim r^2$ in $B_{\text{dis}}(r)$ in Eq. (56). By extension we thus call it the *modified Larkin regime*. In the zero-temperature limit the linear roughness $B_{\text{th}}(r) = \frac{Tr}{c}$ is suppressed and the small lengthscales are dominated by the quadratic term $\sim r^2$, which corresponds to an exponent $\zeta=1$ which is again not the Larkin exponent $\zeta_L|_{d=1} = 3/2$.

D. Crossover at high temperature

At higher temperatures the modified Larkin regime has disappeared, and the intersection of the thermal and the asymptotic roughness, respectively, Eqs. (59) and (62), defines another characteristic crossover length r_*

$$r_* = r_0 \cdot v_c^5 \frac{1}{-\frac{1}{6}\Gamma(-1/5)} \tag{74}$$

and since the value of the cutoff v_c saturates at 5/6 at high T, up to a factor $r_*/r_0 \approx 0.414225$ the crossover r_* is equivalent to the Larkin length r_0. Using Eq. (65) we eventually obtain

$$r_* \overset{T\to\infty}{\approx} \frac{2}{5}\frac{T^5}{cD^2}. \tag{75}$$

This result can be predicted by scaling arguments assuming that there is no intermediate regime between the thermal and the asymptotic Flory-type regimes. This hypothesis is true only in the high-temperature regime, e.g., imposing $\xi=0$ from the beginning (see Sec. VI). This last approximation actually wrongs the low-temperature physics below the Larkin length since it misses the intermediate modified Larkin regime whereas the GVM clearly points out its existence.

E. Alternative formulation of the GVM roughness

We finally give an alternative formulation of the GVM roughness in Eq. (56), starting from Eqs. (51) and (B10), and rescaling in the propagators the energy per Fourier mode $G_c^{-1}(q) = cq^2$ with respect to the mass term at the RSB cutoff $[\sigma](v_c)$. The *ad hoc* changes in variable make explicit the "crossover function" from the thermal to the RM roughness regimes and provide a straightforward way of predicting the temperature dependence of the asymptotic GVM roughness.

The following argument being quite generic, we start with an internal dimension d and a generalized isotropic elasticity indexed by the exponent $\mu>0$ [$\mu=2$ for the usual short-range elasticity in Eq. (4)], which translates into

$$G_c^{-1}(q) = c|q|^\mu \Rightarrow \mathcal{H}_{\text{el}}[u] = \frac{1}{2}\int d^d q\, G_c^{-1}(q) u_{-\vec{q}} u_{\vec{q}}. \tag{76}$$

As seen in Sec. III C, the GVM procedure constrains the form of a full-RSB mass term $[\sigma](u)$ into the following power law ($\nu>0$):

$$[\sigma](u \le v_c) = A_{(c,D)}\left(\frac{u}{T^\psi}\right)^\nu, \quad [\sigma](u \ge v_c) = [\sigma](v_c), \tag{77}$$

where $\nu=10$ and $\psi=1$ in Eq. (37).

The thermal roughness in Eq. (53) generalizes into

$$B_{\text{th}}(r) \equiv \frac{T}{c}\int d^d q \frac{2[1-\cos(\vec{q}\vec{r})]}{|q|^\mu} \sim \frac{T}{c} q^{-(\mu-d)}|_{q\sim 1/r}, \tag{78}$$

i.e., skipping the angular dependence in the cosine's argument

$$B_{\text{th}}(r) \sim \frac{Tr^{2\zeta_{\text{th}}}}{c} \quad \text{with} \quad \zeta_{\text{th}} = \frac{\mu-d}{2}. \tag{79}$$

As for the 'disorder' roughness in Eq. (54), separating the RS ($u \ge v_c$) and full-RSB ($u \le v_c$) segments of $[\sigma](u)$ and

rescaling the energies with respect to $[\sigma](v_c)$ we can apply these two changes in variables

$$\frac{c|q|^\mu}{[\sigma](v_c)} = (r_0|q|)^\mu \equiv |\tilde{q}|^\mu, \quad \text{i.e.,} \quad r_0 \equiv \left[\frac{c}{[\sigma](v_c)}\right]^{1/\mu}, \tag{80}$$

$$\frac{[\sigma](v)}{[\sigma](v_c)} = \left(\frac{v/v_c}{|\tilde{q}|^{\mu/\nu}}\right)^\nu \equiv \tilde{v}^\nu, \quad \text{i.e.,} \quad \tilde{v}|_{v=v_c} = |\tilde{q}|^{\mu/\nu}. \tag{81}$$

We eventually obtain

$$B_{\text{dis}}(r) = \frac{Tv_c^{-1}}{c} r_0^{2\zeta_{\text{th}}} \int d^d\tilde{q} \frac{2[1-\cos(\tilde{q}r/r_0)]}{|\tilde{q}|^\mu} \times \left[\frac{1-v_c}{|\tilde{q}|^\mu + 1} + |\tilde{q}|^{-\mu/\nu} F(|\tilde{q}|^{-\mu/\nu})\right] \tag{82}$$

with the crossover function

$$F(x) \equiv \int_0^x dv \frac{v^{\nu-2}}{1+v^\nu}. \tag{83}$$

As for the cutoffs in the Fourier-modes integral, they are simply redefined with respect to the Larkin length r_0 and are thus harmless at least for the 1D-interface case.

In order to extract the behavior at large lengthscales r, we consider the limit $q \to 0$, i.e., $\tilde{q} \to 0$

$$|\tilde{q}|^{-\mu/\nu} \to \infty \Rightarrow |\tilde{q}|^{-\mu/\nu} \underbrace{F(|\tilde{q}|^{-\mu/\nu})}_{\approx \text{cte}} \approx |\tilde{q}|^{-\mu/\nu}. \tag{84}$$

Thus, by counting in this limit the scaling of $\tilde{q}$ in Eq. (82) we can relate ν to the asymptotic exponent ζ_{asympt} predicted by GVM

$$\tilde{q}^{\,d-\mu-\mu/\nu} \equiv \tilde{q}^{\,-2\zeta_{\text{asympt}}} \Rightarrow \frac{\mu}{\nu} = 2(\zeta_{\text{asympt}} - \zeta_{\text{th}}). \tag{85}$$

We can indeed check that for a 1D interface ($d=m=1$) with short-range elasticity ($\mu=2$) and RB disorder ($\zeta_F = \frac{4-d}{4+m}$), the GVM prediction $\zeta_{\text{asympt}} = \zeta_F = 3/5$, and $\zeta_{\text{th}} = 1/2$ are coherent with $\nu = 10$ of Eq. (41).

This link between ν and ζ_{asympt} can actually be used to predict the temperature dependence of the asymptotic roughness, disregarding the numerical and $A_{(c,D)}$ contributions

$$B(r) \overset{r\to\infty}{\sim} \frac{T}{v_c} r_0^{2\zeta_{\text{th}}} (r/r_0)^{2\zeta_{\text{asympt}}} = \frac{T}{v_c} r_0^{-\mu/\nu} r^{2\zeta_{\text{asympt}}}. \tag{86}$$

Combining Eqs. (80) and (77) we can make explicit the power-law T dependence of r_0 and eventually of the roughness

$$B(r) \overset{r\to\infty}{\sim} T^{1-\psi} v_c^0 r^{2\zeta_{\text{asympt}}}. \tag{87}$$

We can thus conclude immediately that the asymptotic roughness has completely forgotten the interface width ξ since $v_c(\xi)$ has been washed out and that $\psi = 1$ as imposed by the GVM scheme in Sec. III C leads to a T-independent prediction. The elastic constant c has to be T independent to ensure the correct small-lengthscales behavior in Eq. (78) so the only way to modify this last prediction would be to choose a *T-dependent* effective strength of disorder $D(T)$. This will be the case in the second GVM procedure presented in the next section.

V. ROUNDED TOY MODEL: GVM, ROUGHNESS, AND CROSSOVER LENGTHSCALES

The 1D interface, that we have tackled up to now as a static object, can actually be mapped onto a growing, dynamical object, namely, the directed polymer (DP), which consists in an elastic string starting from a basepoint $y=0$ and getting ahead in "time" t in a random potential $\tilde{V}(t,y)$.[23] The weight of a trajectory $y(t')$ of duration t is given by

$$\exp\left(-\beta \int_0^t dt' \left\{\frac{c}{2}[\partial_{t'} y(t')]^2 + \tilde{V}[t', y(t')]\right\}\right) \tag{88}$$

so that through the correspondence $(t,y) \leftrightarrow (z,x)$ one recovers the weight of an interface of "length" $z=t$. The roughness at lengthscale z is for instance recovered from the statistical properties of the DP at finite time t. See also Ref. 43 for another approach.

Our interest goes to finding a simple *approximate* description of the end point $y(t)$ fluctuations, at fixed time t. This allows to determine the average of observables depending on the sole end point position $y(t)$ of the DP (such as the roughness $\overline{\langle [y(t)-y(0)]^2 \rangle}$) but of course not of observables depending on the whole trajectory. The idea is to focus on the effective disorder ruling the extremity of a DP of fixed length.

A. Definition of the rounded toy model

At fixed disorder $\tilde{V}$ and final time t, we approximate the weight $Z_{\tilde{V}}(t,y) = \int \mathcal{D}y' e^{-\beta \mathcal{H}[y', \tilde{V}]}$ of all trajectories $y'(t)$ arriving in y at time t through an effective free energy $F_\eta(t,y) \approx -\beta^{-1} \log Z_{\tilde{V}}(t,y)$, where $\eta = \eta(y)$ is an effective disorder depending only on the arrival position y of the DP

$$F_\eta(t,y) = \frac{c}{2t} y^2 + \int_0^y dy' \cdot \eta(y') + \text{cte}_\eta(t). \tag{89}$$

The first term $\frac{c}{2t} y^2$ is simply the (exact) free energy in the absence of disorder. The t-dependent constant arises from normalization along y while the $\int_0^y \eta$ represents the effective potential experienced by the end point. Ideally, one would infer the distribution of η from that of $\tilde{V}$ but this task is *a priori* extremely difficult at finite time.

However, in the infinite-time limit, it is known[23] that the exact correlator $\langle [F(t,y_2) - F(t,y_1)]^2 \rangle$ is proportional to $|y_2 - y_1|$, as provided, e.g., by η being a delta-correlated white noise. For finite-time, numerical evidence[44] support that this correlator still behaves as $|y_2 - y_1|$ at short distance, and it has been proposed[45,46] that taking a delta-correlated white noise for η in Eq. (89) indeed provides an approximate but good description of the DP end-point statistics.

In order to tackle the question of the influence of finite disorder correlation length on the properties of an interface,

it is thus very natural to examine in details the corresponding model in which the delta-correlated noise η is now replaced by a white noise with Gaussian correlations of width $\tilde{\xi}$ and effective strength $\tilde{D}$

$$\overline{\eta(y)} = 0, \quad \overline{\eta(y)\,\eta(y')} = \tilde{D} \cdot R_{\tilde{\xi}}(y - y')|_{D=1} \tag{90}$$

[see Eq. (8) for the definition of the correlator $R_{\tilde{\xi}}$]. The limit $\tilde{\xi} \to 0$ yields a delta-correlated disorder and corresponds to the original so-called toy model.[47] A finite $\tilde{\xi}$ actually rounds the correlator of the free energy $F(t,y)$ around $y=0$.

These properties thus define a modified "rounded" toy model, in which the average of an observable $\mathcal{O}$ writes

$$\langle \mathcal{O}(t) \rangle_\eta = \frac{\int dy \cdot \mathcal{O}(t,y) e^{-\beta F_\eta(t,y)}}{\int dy\ e^{-\beta F_\eta(t,y)}}. \tag{91}$$

Although much more simple than the full interface model, since the fluctuations are now reduced to those of the end point instead of the total interface, our rounded toy model is still not tractable in an exact way, and we resort to the GVM approximation in the replica approach. We follow here the route used for a previous modified toy model in Ref. 48 (in which was assumed a power-law asymptotic decay of the disorder correlator). Having reduced the dimension of the model from the directed polymer to the toy model, we hope that the GVM method catches exact scaling exponents at small and large times, together with crossover lengthscales.

Introducing replicas and averaging over disorder one gets the analog of Eq. (12)

$$\overline{\langle \mathcal{O}(t) \rangle} = \lim_{n \to 0} \int dy_1 (\cdots) dy_n \cdot \mathcal{O}(t,y_1) e^{-\beta \tilde{F}(t,\vec{y})} \tag{92}$$

with the effective free energy

$$\tilde{F}(t,\vec{y}) = \frac{c}{2t} \sum_{a=1}^{n} y_a^2 - \frac{\beta \tilde{D}}{2} \sum_{a,b=1}^{n} \min\nolimits_{\tilde{\xi}}(y_a, y_b), \tag{93}$$

where at $\tilde{\xi}=0$ (i.e., for η a delta-correlated white noise), $\min_{\tilde{\xi}}$ would be the minimum function. At finite $\tilde{\xi}$ it actually writes

$$\min\nolimits_{\tilde{\xi}}(y_a, y_b) = \frac{1}{2}(y_a + y_b - |y_a - y_b|_{\tilde{\xi}}) \tag{94}$$

$|y|_{\tilde{\xi}}$ is the absolute value function, rounded close to the origin. In Fourier representation, it reads

$$|y|_{\tilde{\xi}} = \int_{\mathbb{R}} d\lambda \cdot \frac{2[1 - \cos(\lambda y)]}{\lambda^2} e^{-\lambda^2 \tilde{\xi}^2}. \tag{95}$$

Note that we have not given a definite value to the strength $\tilde{D}$ of the effective disorder $\eta(y)$. To fit the infinite-time exact result[23] for $\langle [F(t,y_2) - F(t,y_1)]^2 \rangle$, one has to take

$$\tilde{D} = \frac{cD}{T}. \tag{96}$$

This ensures in particular that the disorder strength D of the full model [see Eq. (2)] has the same dimensions as the constant D of Eq. (96) for the toy model. In addition, the expression (96) tells us that the disorder contribution to the effective free-energy $F_\eta(t,y)$ in Eq. (89) *depends on temperature*, which is in a way expected since it is aimed at representing the contribution of all trajectories arriving at the end point, each trajectory being sensitive to thermal fluctuations.

B. GVM and determination of $\sigma(u)$ and $[\sigma](u)$

To determine the roughness at all times t we follow the lines of Sec. III A. The main difference is that we work in direct space at fixed t so that there are no Fourier transformations to consider, and the GVM solution depends on time t (i.e., of the lengthscale r in the 1D-interface formulation). The equivalent of the trial Hamiltonian is provided by the quadratic trial free energy

$$F_0(t,\vec{y}) = \frac{1}{2} \sum_{a,b=1}^{n} y_a G_{ab}^{-1}(t) y_b \tag{97}$$

parametrized by a $n \times n$ hierarchical matrix whose elements are

$$G_{ab}^{-1}(t) = c/t \cdot \delta_{ab} - \sigma_{ab}. \tag{98}$$

The diagonal term c/t corresponds to the elastic part of the free energy while the off-diagonal elements σ_{ab} do not depend on t since $\tilde{F}$ is local in time. The variational method yields the following disorder-independent connected parts:

$$G_c^{-1}(t) = c/t \Leftrightarrow G_c(t) = t/c \tag{99}$$

thanks to the statistical tilt symmetry as in Eqs. (28) and (29), together with self-consistent saddle-point equations for the off-diagonal elements

$$\sigma_{a \neq b} = \frac{\tilde{D}}{\sqrt{\pi} T} \{ \tilde{\xi}^2 + T[\tilde{G}(t) - G_{a \neq b}(t)] \}^{-1/2}. \tag{100}$$

The above is equivalent to the saddle point Eq. (32) of the full interface but with two important differences: (i) there is no integration over Fourier modes q since we work in a direct space representation and (ii) the exponent is $-1/2$ instead of $-3/2$, and thus leads to a different asymptotic behavior.

As in Sec. III B we use the more generic full-RSB formulation with the mapping parameter $u \in [0,1]$

$$\sigma(u) = \frac{\tilde{D}}{\sqrt{\pi} T} \{ \tilde{\xi}^2 + T[\tilde{G}(t) - G(t,u)] \}^{-1/2}. \tag{101}$$

Following the same procedure as in Sec. III C, we obtain

$$\sigma'(u) = \sigma'(u) \frac{(T\sigma(u))^3}{[G_c^{-1}(t) + [\sigma](u)]^2} \frac{\pi}{2\tilde{D}^2}. \tag{102}$$

If we are not on a plateau $\sigma'(u)=0$, we thus obtain

$$T\sigma(u) = \left(\frac{2\tilde{D}^2}{\pi}\right)^{1/3} [G_c^{-1}(t) + [\sigma](u)]^{2/3}. \tag{103}$$

Taking again the derivative ∂_u on this last expression, in order to reintroduce a u dependence, and identifying $\sigma(u)$ with respect to $[G_c^{-1}+[\sigma](u)]$, we obtain

$$\sigma(u) = \frac{2^3}{3^2\pi}\frac{\tilde{D}^2}{T}(u/T)^2, \tag{104}$$

$$[\sigma](u) = \frac{2^4}{3^3\pi}\tilde{D}^2(u/T)^3 - G_c^{-1}(t), \tag{105}$$

where we recognize the same power-law structure $(u/T)^\nu$, imposed by the very GVM procedure, as in Eqs. (37) and (38), respectively, for $[\sigma](u)$ and $\sigma(u)$. However the effective strength of disorder $\tilde{D}$ given by Eq. (96) allows to modify this temperature dependence and thus to circumvent the GVM artifact which leads to a T-independent asymptotic roughness for the 1D-interface GVM (see Sec. VI). Moreover, contrarily to Eq. (38) there is no additive constant to $\sigma(u)$, the GVM in direct space provides indeed both the solution for $\sigma(u)$ and $[\sigma](u)$. In the Fourier representation we obtained first $[\sigma](u)$ and then had to integrate it to recover $\sigma(u)$, which was leading to an additive constant. As a consequence the solution $\sigma(u)$ has to stick to these power-law functions with possible steps and plateaux in between monotonous segments.

As for the GVM of the 1D interface, we look for a full-RSB *continuous* solution, without any additional step. In fact, by definition $[\sigma](0)=0$ and consequently this imposes the existence of a plateau for u below a first cutoff $u_*(t)$ which introduces the lengthscale dependence into the solution and later on into the roughness via the connected part in Eq. (99)

$$u_*(t) = \frac{3}{2}\left(\frac{\pi c}{2\tilde{D}^2}\right)^{1/3} T\, t^{-1/3}, \tag{106}$$

$$[\sigma](u \le u_*) \equiv [\sigma](0) = 0. \tag{107}$$

$$\sigma(u \le u_*) = \sigma(0) = \left(\frac{2\tilde{D}^2c^2}{\pi}\right)^{1/3} T^{-1}t^{-2/3}. \tag{108}$$

The consistency of Eq. (101) for $u \ge u_*$ imposes the existence of a second cutoff $u_c(\tilde{\xi})$ above which $\sigma(u)$ has a plateau, similarly to Eq. (43). Indeed, using the inversion formula (B11) for $u_* \le u \le u_c$ and taking care of the two plateaux in $\int_u^1 dv$, the saddle point Eq. (101) requires again that the $\tilde{\xi}$ dependence cancels the u_c terms as in Eq. (45). We thus obtain the following polynomial equation for the second full-RSB cutoff $u_c(\tilde{\xi})$ similarly to Eq. (45):

$$u_c^4 = \tilde{A}(3/4 - u_c),$$

$$\tilde{A} \equiv \frac{3^3}{2^4}\pi \cdot \frac{T^4}{(\tilde{\xi}\tilde{D})^2} = \frac{3^3}{2^4}\pi \cdot \frac{T^6}{(\tilde{\xi}cD)^2}, \tag{109}$$

which is equivalent to substituting Eqs. (104) and (105) into Eq. (101) at $u=u_c$. As for the GVM of the 1D interface, it can be shown that the factor 3/4 is closely related to the GVM prediction for the asymptotic roughness exponent, which in the case of the toy model will be the exact random manifold exponent for a 1D interface: $u_c < 3/4 = (2\zeta_{\mathrm{RM}})^{-1}$.

An explicit analytical expression for $u_c \in [0,3/4]$ can be obtained for the two opposite limits for $\tilde{A}$, which at fixed $\tilde{\xi},\tilde{D}>0$ correspond, respectively, to $T\to 0$ and $T\to\infty$

$$u_c \overset{\tilde{A}\to 0}{\approx} \frac{3\pi^{1/4}}{2^{3/2}}\frac{T}{(\tilde{\xi}\tilde{D})^{1/2}} = \frac{3\pi^{1/4}}{2^{3/2}}\frac{T^{3/2}}{(\tilde{\xi}cD)^{1/2}} \to 0, \tag{110}$$

$$u_c \overset{\tilde{A}\to\infty}{\approx} 3/4 + 0^-. \tag{111}$$

The polynomial equation for $u_c(\tilde{\xi})$ (109) leads to the analogous definition of a characteristic temperature with respect to Eq. (48) between the low- and high-temperature regimes, using Eq. (96)

$$\tilde{A} = 1 \Leftrightarrow \frac{T_c}{(\tilde{\xi}cD)^{1/3}} = \left(\frac{2^4}{3^3\pi}\right)^{1/6} \approx 0.76 \tag{112}$$

and this last constant is of order 1. This criterion shows again that the limits of the different parameters, in particular, $T\to 0$ and $\xi\to 0$ cannot be exchanged. Moreover the scaling between the parameters $\{T,\tilde{\xi},D\}$ is exactly the same as in Eq. (48) for the GVM on the 1D interface.

Using the inversion formulas of hierarchical matrices in $\lim_{n\to 0}$, the physically relevant parameters are $[\sigma](u)$ and $\sigma(0)$ so this full-RSB solution can be summarized by

$$\sigma_{\mathrm{RSB}}(0) = \left(\frac{2\tilde{D}^2c^2}{\pi}\right)^{1/3} T^{-1}t^{-2/3},$$

$$[\sigma]_{\mathrm{RSB}}(u \le u_*) = [\sigma]_{\mathrm{RSB}}(u \ge u_c) = 0,$$

$$[\sigma]_{\mathrm{RSB}}(u_* \le u \le u_c) = \frac{2^4}{3^3\pi}\tilde{D}\,(u/T)^3 - c/t. \tag{113}$$

To be consistent the Ansatz must also satisfy $0 \le u_*(t) < u_c(\tilde{\xi}) \le 3/4$ and the collapse of those two cutoffs actually defines the lowest time t_c for the existence of a full-RSB segment in the solution

$$u_*(t_c) \equiv u_c(\tilde{\xi}). \tag{114}$$

This condition is equivalent to $[\sigma](u_*(t_c)) = [\sigma](u_c(\tilde{\xi}))$ and can be reformulated as

$$t_c = \frac{3^3\pi}{2^4}\frac{c}{\tilde{D}^2}\left(\frac{T}{u_c}\right)^3 = \frac{3^4\pi}{2^6}\frac{cT^3}{\tilde{D}^2}u_c^{-4} - \frac{c\tilde{\xi}^2}{T}. \tag{115}$$

This crossover time can be made explicit in the two limits in Eqs. (110) and (111) plugged in Eq. (106). This gives, respectively,

$$t_c \overset{\tilde{A}\to 0}{\approx} 2^{1/2}\pi^{1/4}\cdot\tilde{\xi}^{3/2}c\tilde{D}^{-1/2}, \tag{116}$$

$$t_c \overset{\tilde{A}\to\infty}{\approx} 4\pi\frac{T^3 c}{\tilde{D}^2}. \tag{117}$$

For smaller lengthscales $t \le t_c$ the two plateaux merge into a RS Ansatz. Following Eqs. (B5) and (99), we have then $\tilde{G}(t)-G(t,u)=G_c(t)=t/c$ and the saddle-point Eq. (101) becomes

$$\sigma_{\mathrm{RS}}(u) = \sigma_{\mathrm{RS}}(0) = \frac{\beta\tilde{D}}{\sqrt{\pi}}\left(\tilde{\xi}^2 + \frac{Tt}{c}\right)^{-1/2},$$

$$[\sigma]_{\mathrm{RS}}(u) = 0. \tag{118}$$

So the GVM in direct space of the DP toy model yields a solution of the saddle-point Eq. (101) which depends explicitly on the time t, and consequently on the length of the DP; it is RS for $t \le t_c$ and becomes continuously full-RSB with two plateaux for $t \ge t_c$. This is summarized in Fig. 5. The breaking of the replica symmetry at $t=t_c(\tilde{\xi})$ has the same source as the full-RSB cutoff $v_c(\xi)$ in the GVM of the 1D interface: it marks the transition from a small-lengthscales regime where the DP starts by fluctuating thermally and crosses smoothly over to the large-lengthscales RM regime where the disorder-induced metastability is dominant.[48] In the next section we compute the corresponding roughness, which also gives access to the actual crossover from the thermal to the RM regime depending on the explicit finite width $\tilde{\xi}$.

C. Computation of the roughness

The roughness of the 1D interface in Eq. (15) translates into the transverse fluctuations of the DP's end point $\overline{\langle[y(t)-y(0)]^2\rangle}$ and since $y(0)\equiv 0$ the corresponding GVM correlation function is given by

$$\overline{\langle y(t)^2\rangle} = T\lim_{n\to 0}\tilde{G}(t). \tag{119}$$

Using the inversion formula (B10) we eventually obtain

$$t \ge t_c:\ \lim_{n\to 0}\tilde{G}(t) = \frac{3}{2}\left(\frac{2\tilde{D}^2}{\pi c^4}\right)^{1/3} t^{4/3} - \tilde{\xi}^2, \tag{120}$$

$$t \le t_c:\ \lim_{n\to 0}\tilde{G}(t) = \frac{Tt}{c} + \frac{\tilde{D}}{c^2\sqrt{\pi}}\cdot t^2\left(\tilde{\xi}^2 + \frac{Tt}{c}\right)^{-1/2}. \tag{121}$$

We can check that this quantity and its derivative are continuous, in particular at the junction of the RS and full-RSB solutions

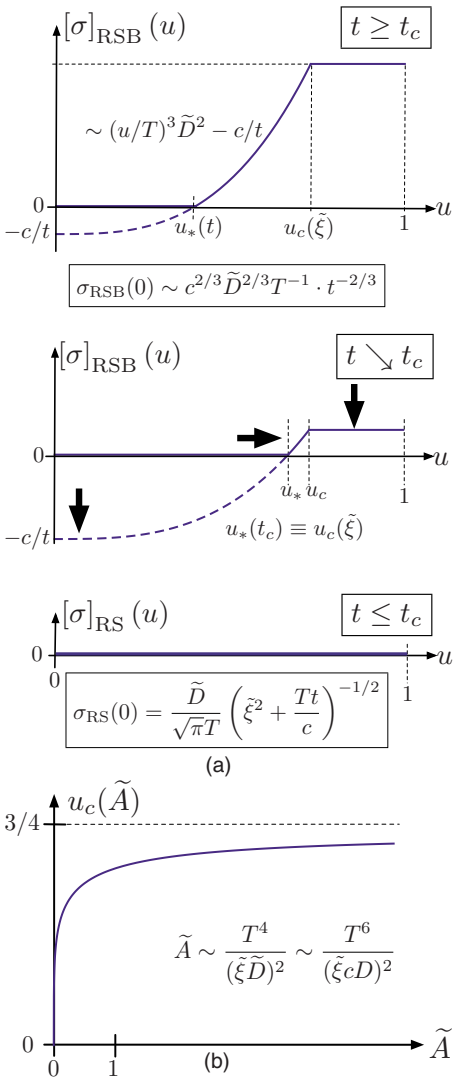

FIG. 5. (Color online) GVM solution for the toy model. (a) Self-energy $[\sigma](u)$ given by Eq. (113). At large times (large lengthscales) $t \ge t_c$ it is full-RSB with two plateaux which merge at $t=t_c$, as indicated by the black arrows, and at small times (small lengthscales) $t \le t_c$ it is RS. (b) Full-RSB cutoff u_c as a function of $\tilde{A} \sim \frac{T^4}{(\tilde{\xi}\tilde{D})^2} \sim \frac{T^6}{(\tilde{\xi}cD)^2}$, obtained by solving the polynomial Eq. (109). It starts linearly at $\tilde{A} \to 0$ and saturates to 3/4 at $\tilde{A} \to \infty$ similarly to Fig. 2(b) but $\tilde{D}=\tilde{D}(T)$ will modify its low-temperature dependence in Eq. (110).

$$\lim_{n\to 0}\tilde{G}_{\mathrm{RS}}(t_c) = \lim_{n\to 0}\tilde{G}_{\mathrm{RSB}}(t_c) = \tilde{\xi}^2\cdot\frac{3/2+u_c}{3/4-u_c}, \tag{122}$$

$$\partial_t \lim_{n\to 0}\tilde{G}_{\mathrm{RS}}(t)\big|_{t=t_c} = \partial_t \lim_{n\to 0}\tilde{G}_{\mathrm{RSB}}(t)\big|_{t=t_c} = \frac{3T}{u_c}. \tag{123}$$

In order to compare the GVM predictions for the 1D interface and the rounded toy model, we use Eq. (96) to recover the physical temperature dependence of $\tilde{D}$ and we identify

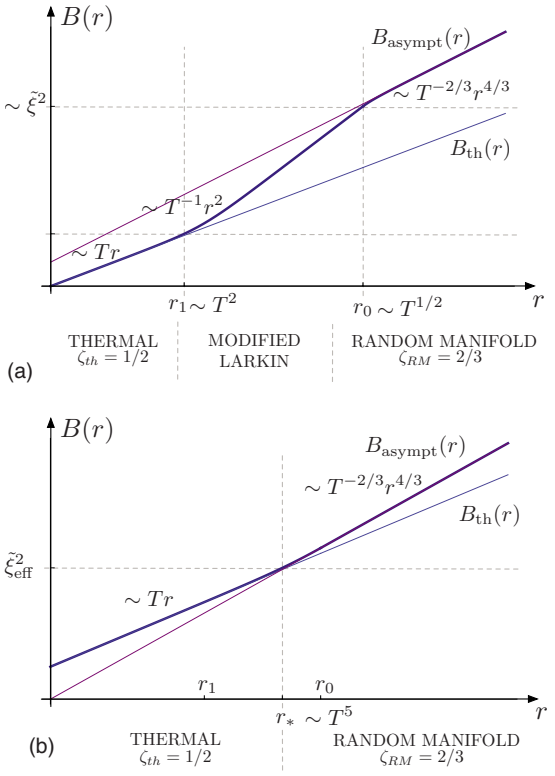

FIG. 6. (Color online) GVM prediction for the toy-model static roughness $B(r)$, in log-log representations; the slope of the curves corresponds to $2\zeta(r)$ as defined by Eq. (17). It can be compared to Fig. 3 [$\tilde{\xi}=c=D=1$, (a) $T=10^{-3}$, and (b) $T=10$].

$$r_0 = t_c, \quad B(r) = \overline{\langle y(t)^2 \rangle}|_{t=r}. \tag{124}$$

Keeping track of the RS and full-RSB solution we obtain the roughness predicted by GVM on the toy model

$$r \geq r_0\text{: } B_{\mathrm{RSB}}(r) = \frac{3}{2}\left(\frac{2D^2}{\pi c^2 T^2}\right)^{1/3} r^{4/3} - \tilde{\xi}^2, \tag{125}$$

$$r \leq r_0\text{: } B_{\mathrm{RS}}(r) = \frac{Tr}{c} + \frac{D}{cT\sqrt{\pi}} r^2 \left(\tilde{\xi}^2 + \frac{Tr}{c}\right)^{-1/2} \tag{126}$$

with the characteristic lengthscale associated to the full-RSB cutoff $u_c(\tilde{\xi})$ in Eq. (109)

$$r_0 = \frac{3^3\pi}{2^4}\frac{T^5}{cD^2} u_c^{-3}. \tag{127}$$

This length differs from Eq. (58) essentially by the scaling of u_c.

We show in Fig. 6 two graphs illustrating the low- versus high-temperature regimes of $B(r)$. A summary of the different roughness regimes along with their corresponding exponent ζ and their crossover lengthscales is given by Fig. 8(b).

D. Roughness regimes and crossover lengthscales

We recover at small lengthscales the same thermal regime of exponent $\zeta_{\mathrm{th}}=1/2$ as in Sec. IV A 1 whereas at large lengthscales the power-law behavior is directly given by Eq.

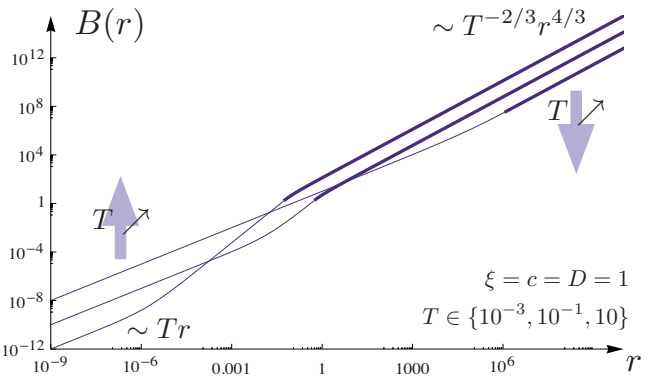

FIG. 7. (Color online) GVM roughness at fixed disorder for the toy model, on four orders of magnitude for the temperature: the thick curves correspond to $B_{\mathrm{RSB}}(r)$, the thin ones to $B_{\mathrm{RS}}(r)$, and they connect at the Larkin length r_0. Unlike Fig. 4(b) the curves intersect because of the asymptotic scaling $\sim T^{-2/3}$ and become thus unphysical in the zero-temperature limit.

(125) which predicts the *exact* RM exponent $\zeta_{\mathrm{RM}}=2/3$ of a 1D interface instead of the Flory exponent $\zeta_F=3/5$ obtained in Sec. IV A 2. Note that $\zeta_{\mathrm{RM}}=2/3$ coincides with an exact prediction for the original toy model ($\tilde{\xi}=0$).[39] This leads in particular to an asymptotic temperature-dependence $\sim T^{-2/3}$, which makes the $B(r)$ curves intersect with each other upon varying T, as illustrated by Fig. 7.

As in Sec. IV B the lengthscale $r_0=t_c$ corresponds to the Larkin length of the system (associated to the appearance of full RSB), at least if we define an effective width $\tilde{\xi}_{\mathrm{eff}}$ at high temperatures. Indeed, the expansions (116) and (117) give the following analytical expressions for r_0:

$$r_0 \overset{T\to 0}{\approx} 2^{1/2}\pi^{1/4} \cdot \tilde{\xi}^{3/2} c D^{-1/2} T^{1/2}, \tag{128}$$

$$r_0 \overset{T\to\infty}{\approx} 4\pi \frac{T^5}{cD^2}, \tag{129}$$

which, when compared to Eq. (64) and, respectively, to Eq. (65) predicts exactly the same scaling of parameters at high temperatures but introduces a temperature dependence $\sim T^{1/2}$ and slightly modifies the scaling-exponents values at low temperatures. Combining Eq. (122) with Eq. (109) the roughness at r_0 is given by

$$B(r_0) = \tilde{\xi}^2 \cdot \frac{3/2 + u_c}{3/4 - u_c} = \frac{3^3}{2^4}\pi \frac{T^6}{(cD)^2} u_c^{-4}, \tag{130}$$

so we have, respectively, in the two opposite temperature limits in Eqs. (110) and (111)

$$B(r_0) \overset{T\to 0}{\approx} \frac{1}{2}\tilde{\xi}^2, \tag{131}$$

$$B(r_0) \overset{T\to\infty}{\approx} \frac{2^4}{3}\pi \frac{T^6}{(cD)^2} \equiv \tilde{\xi}^2_{\mathrm{eff}}. \tag{132}$$

Remarkably, except for the numerical factors, both these expressions are strictly equivalent to Eqs. (67) and (69) ob-

tained in the previous GVM procedure. This is compatible with a generic scaling analysis of the model (see Sec. VI).

Below the Larkin length the roughness is described by the RS solution

$$B_{\mathrm{RS}}(r) = B_{\mathrm{th}}(r) + \frac{\tilde{\xi}^3 cD}{\sqrt{\pi} T^3} f(r/r_c),$$

$$r_c \equiv c\tilde{\xi}^2/T \Leftrightarrow B_{\mathrm{th}}(r_c) = \tilde{\xi}^2,$$

$$f(x) = \frac{x^2}{\sqrt{1+x}}, \tag{133}$$

where the dimensionless $f(x)$ describes the actual shape of the crossover along with the definition of r_c. The thermal roughness obtained from the rounded toy model differs on two points from its counterpart for the 1D interface, as a consequence of the GVM in direct-space versus Fourier representation: (i) the RS solution encodes both the thermal and the intermediate crossover regimes, instead of the thermal regime only and (ii) the crossover function is given explicitly after the retrieval of the thermal roughness, whereas in Eq. (56) it was given as a series. Taylor expanding $f(x)$ around $x=0$, we have

$$B(r) \overset{r\to 0}{\approx} \frac{Tr}{c} + r^2 \frac{D}{\sqrt{\pi}\tilde{\xi} cT} - r^3 \frac{D}{2\sqrt{\pi} c^2 \tilde{\xi}^3} + \mathcal{O}(Tr^4) \tag{134}$$

so the end of the thermal regime can be defined similarly to Eq. (71) as the quadratic take-off $\sim r^2$

$$\frac{Tr_1}{c} \equiv r_1^2 \frac{D}{\sqrt{\pi}\tilde{\xi} cT} \Leftrightarrow r_1 = \frac{T^2 \tilde{\xi}}{\sqrt{\pi} D}. \tag{135}$$

The collapse of r_1 and r_0 yields the analogous criterion to Eq. (73) for a characteristic temperature

$$r_1 = r_0 \Leftrightarrow u_c = \frac{3\pi^{1/6}}{2^{4/3}} \frac{T}{(\tilde{\xi} cD)^{1/3}}, \tag{136}$$

which is compatible with the previous criterion of Eq. (112) on the GVM solution itself.

As for the zero-temperature limit, it is ill-defined, since $r_0 \to 0$ and $B_{\mathrm{dis}}(r_0)$ is finite in Eq. (131), whereas its derivative and $B_{\mathrm{RSB}}(r)$ itself clearly diverge according to Eqs. (123) and (126). The toy model is actually an effective model at *finite* temperature and is thus nonphysical for this particular limit.

Finally at high temperatures there is a single crossover lengthscale between the thermal and the RM regime, denoted r_* and scaling as Eq. (74)

$$\frac{Tr_*}{c} \equiv \frac{3}{2}\left(\frac{2D^2}{\pi c^2 T^2}\right)^{1/3} r_*^{4/3} \Leftrightarrow r_* = \frac{4\pi}{27} \frac{T^5}{cD^2}, \tag{137}$$

which is equivalent up to a factor 1/27 to the Larkin length r_0 at high temperatures and can be predicted by scaling arguments.

VI. SCALING ANALYSIS

In order to explain the universal expressions of T_c, r_0, and ξ_{eff}, we follow in spirit the scaling analysis presented in Refs. 28 and 29 but keeping ξ finite. We fully harness the scaling relations of the Hamiltonian and the roughness so as to derive identities between different scaling exponents, and also to show how the Flory exponent ζ_F arises naturally even if the so-called Flory argument (see Appendix A) does not apply. In particular, we account for the role of the GVM approximation in those scalings, for both the 1D interface and the rounded toy model.

For the sake of generality, we consider a manifold of internal dimension d with m transverse components, subjected to a random-bond potential $\tilde{V}$. The weight of one configuration reads (see Sec. II A)

$$\int \mathcal{D}u \exp\left\{-\beta \int d^d z \left[\frac{c}{2}[\nabla_z u(z)]^2 + \tilde{V}(u(z),z)\right]\right\}. \tag{138}$$

The distribution of $\tilde{V}$ is assumed to be Gaussian with correlations

$$\overline{\tilde{V}(u,z)\tilde{V}(u',z')} = D\frac{1}{\xi^m} R\left(\frac{u-u'}{\xi}\right)\delta^{(d)}(z-z') \tag{139}$$

ξ being the microscopic disorder correlation length and R a dimensionless function. Let's perform the change of variable

$$u = a\bar{u} \quad z = b\bar{z}. \tag{140}$$

We note that the elastic part of the Hamiltonian rescales as

$$\int d^d z \frac{c}{2}(\nabla_z u)^2 = b^{d-2}a^2 \int d^d \bar{z} \frac{c}{2}(\nabla_{\bar{z}} \bar{u})^2 \tag{141}$$

while (in distribution) the disorder part rewrites

$$\int d^d z \tilde{V}(u,z) = b^{d/2} a^{-m/2} \int d^d \bar{z} \bar{V}(\bar{u},\bar{z}), \tag{142}$$

where $\bar{V}$ has a microscopic correlation length ξ/a. Searching for a *unique* exponent ζ such that $a=b^\zeta$ and such that the elastic and the disorder parts of the Hamiltonian both scale in the same way, we find

$$\zeta = \zeta_F = \frac{4-d}{4+m}. \tag{143}$$

Starting from the definition of the roughness

$$B(z) = \int \mathcal{D}\tilde{V} \frac{P[\tilde{V}]}{Z_{\tilde{V}}} \int \mathcal{D}u [u(z)-u(0)]^2 e^{-\beta \mathcal{H}[u,\tilde{V}]} \tag{144}$$

and denoting

$$\chi_F = 2(\zeta_F - \zeta_{\mathrm{th}}) \tag{145}$$

(one has $\zeta_{\mathrm{th}} = \frac{2-d}{2}$ in the short-range elastic case, and $\chi_F > 0$), one eventually obtains that the roughness obeys the following scaling relation:

$$B(z;c,D,T,\xi) = b^{2\zeta_F} B(b^{-1}z;c,D,b^{-\chi_F}T,b^{-\zeta_F}\xi). \quad (146)$$

Note that this scaling relation also holds in the GVM approach for the interface: indeed, the replicated Hamiltonian (13) and thus its quadratic GVM equivalent in Eq. (18) both rescale in the same way as the original Hamiltonian upon Eq. (140) with $a=b^{\zeta_F}$ as implied by the scaling of the elastic contribution $G_c^{-1}(q)=cq^2$.

In a high-temperature regime the thermal fluctuations wash out the presence of ξ and thus the roughness is expected to be ξ independent. It follows that one can probe a scale-invariant behavior (e.g., at small or large z) of the form

$$B(z) \sim \text{cte}\, T^{2\flat} z^{2\zeta}, \quad (147)$$

where we have isolated the T dependence of the prefactor of $z^{2\zeta}$, defining the *thorn* exponent $\flat$. Choosing $b=T^{1/\chi_F}$ we obtain from Eq. (146) that in each regime where the scaling law in Eq. (147) applies, the following relation holds:

$$\flat = \frac{\zeta_F - \zeta}{\chi_F}. \quad (148)$$

This last relation is always verified in the thermal regime (at small lengthscales z), where $\zeta=\zeta_{\text{th}}=\frac{2-d}{2}$ which from Eq. (145) yields $\flat_{\text{th}}=\frac{1}{2}$ as expected. Denoting by ζ_{RM} the roughness exponent at large z, one has, in particular,

$$\flat_{\text{RM}} = \frac{\zeta_F - \zeta_{\text{RM}}}{\chi_F}. \quad (149)$$

Note however that any relevance of ξ would *a priori* add a T-dependent prefactor to the power-law behavior in Eq. (147). In the large z regime, the value of ζ depends on the model details for disorder: we note for instance that Eq. (149) is verified in the 1D-interface GVM approach, where as noted previously the roughness is then temperature-independent at large scale ($\flat_{\text{RM}}^{\text{1D}}=0$) and the roughness exponent arising from the computation is $\zeta_{\text{RM}}^{\text{1D}}=\zeta_F$ whereas the exact value $\zeta_{\text{RM}}^{\text{exact}}=2/3$ predicts for (149) $\flat=-\frac{1}{3}$ which is compatible with the numerical simulations of Ref. 29.

Our previous considerations are based on exact relations—forgetting about cutoffs in Fourier modes—arising from scaling. Let's now examine the (usually approximate) Flory argument and determine how it fails to gives the correct ζ_{RM} for the 1D interface. It consists again in searching for an exponent ζ such that $a=b^{\zeta}$ and such that the elastic in Eq. (141) and the disorder in Eq. (142) parts of the Hamiltonian both scale in the same way, *and* in assuming scale invariance, i.e., that the roughness is a unique power law $B(z) \sim a^{2\zeta_F} \sim z^{2\zeta_F}$ at all lengthscales, for $b=z$ absorbing all z dependence through Eq. (140)—see also Appendix A. We see however that indeed taking $b=z$ in Eq. (146), one would find $\zeta_{\text{RM}}=\zeta_F$ for large z if it were true that $B(1;c,D,z^{-\chi_F}T,z^{-\zeta_F}\xi)$ was independent of z for large z. This last assumption is however wrong since in general $\flat \neq 0$.

The scaling arguments we have explicited above can also be extended as follows: we now search in Eq. (146) for a and b functions of c, D, and T so as to absorb in $\beta\mathcal{H}$ all the dependence in c, D, and T. We first notice that the random potential scales in distribution as

$$\tilde{V}(u,z) = a^{-m/2} b^{-d/2} \bar{V}(\bar{u},\bar{z}), \quad (150)$$

where $\bar{V}$ is a random potential of Gaussian distribution with D-independent variance and of microscopic correlation length $\bar{\xi}=\xi/a$, or in other words $\bar{V}(\bar{u},\bar{z})\bar{V}(\bar{u}',\bar{z}') = \bar{\xi}^{-m} R[(\bar{u}-\bar{u}')/\bar{\xi}]\delta^{(d)}(\bar{z}-\bar{z}')$. Then one checks that $\beta\mathcal{H}[u,V]=\mathcal{H}[\bar{u},\bar{V}]|_{c=D=1}$ is fulfilled provided (see also Ref. 29) that

$$a = (c^{-d} D^{d-2} T^{4-d})^{1/[(4+m)\chi_F]} \quad b = (c^{-m} D^2 T^{4+m})^{1/[(4+m)\chi_F]}. \quad (151)$$

This yields the scaling form

$$B(z;c,D,T,\xi) = a^2 B_1(b^{-1}z;a^{-1}\xi), \quad (152)$$

where $B_1(\bar{z};\bar{\xi})$ is the roughness at distance $\bar{z}$ with $c=D=T=1$ and disorder correlation length $\bar{\xi}$. Let's examine the information contained in the scaling form (152), which holds for both the interface and the toy model with or without GVM, as directly checked. We first note that if $a^{-1}\xi$ is small enough, the existence of a small disorder correlation length can be ignored; this defines a characteristic temperature

$$T_c = c^{d/(4-d)} D^{(2-d)/(4-d)} \xi^{\chi_F/\zeta_F} \quad (153)$$

above which the effects of ξ should be irrelevant. For the 1D interface ($d=m=1$), one recovers indeed the same characteristic temperature $T_c \sim (\xi c D)^{1/3}$ of Eqs. (48) and (112), respectively, for the 1D interface and rounded toy-model GVM approaches.

Besides, in the now well-defined high-temperature regime $T>T_c$ the roughness should scale as $B(z;c,D,T) = a^2 B_1(b^{-1}z)$ independently of ξ, and display two asymptotic regimes with no intermediate regime (see Ref. 29 for a numerical study). The Larkin length r_0 at which the thermal and random manifold regimes connect can be directly inferred from Eqs. (151) and (152), and is remarkably *independent* on the actual values of ζ_{th} and ζ_{RM}. Indeed r_0 is solution of $a(b^{-1}r_0)^{2\zeta_{\text{th}}} = a(b^{-1}r_0)^{2\zeta_{\text{RM}}}$ which gives $r_0=b$. One recovers the same $\frac{T^5}{cD^2}$ behavior of Eq. (75) for the GVM of the 1D interface and of Eq. (137) for the GVM of the rounded toy model. Similarly the value $\xi_{\text{eff}}^2 \equiv B(r_0)$ of the roughness at this length is independent of both exponents: $\xi_{\text{eff}}=a$. This yields $\xi_{\text{eff}}=\frac{T^3}{cD}$ as indeed obtained both in the interface in Eq. (70) and the toy model in Eq. (132) GVM approaches, even though they do not share the same value for ζ_{RM}. In the low-temperature phase $T<T_c$ however, having more than one characteristic lengthscale, the previous argument does not apply and indeed we have observed that the low-temperature Larkin length r_0 differ between the two GVM predictions for the interface and the toy model.

One has to make an important observation about applying to the toy model the scaling arguments exposed at the beginning of this section. The Flory exponent ensuring that both parts of the Hamiltonian scale identically is $\zeta_F^{\text{toy}}=\frac{2}{3}$ instead of Eq. (143) ($\zeta_F^{\text{toy}}=\frac{2}{3}$ as assumed in the formal argument of Appendix A). Applying blindly Eq. (149), one would infer that $\flat^{\text{toy}}=0$, whereas the thorn exponent for the toy model has the

correct value $\hat{p}^{\text{toy}}=-\frac{1}{3}$. To understand this, one has to remark that Eq. (146) is true if we replace D by $\tilde{D}=\frac{cD}{T}$, which induces an additional T dependence ensuring $\hat{p}^{\text{toy}}=-\frac{1}{3}$. In a nutshell, we just pointed that it is the T dependence of the effective disorder $\tilde{D}$ seen by the DP end point in the toy model which allows for the Flory argument and the GVM method to yield the correct ζ_{RM} and $\hat{p}_{\text{RM}}$ exponents. Note that nevertheless Eqs. (151) and (152) hold without restriction for the toy model.

VII. DISCUSSION

A. Low- and high-temperature regimes

In the previous sections we have determined under various approximation schemes the expression of the roughness $B(r)$, not only in the asymptotic regimes but also on the whole range of scales r. We have kept the disorder correlation length ξ finite, and it is now time to fit the pieces of the puzzle together and analyze its role.

An important quantity that has come to light is the characteristic temperature (defined here disregarding numerical factors)

$$T_c \equiv (\xi c D)^{1/3} \tag{154}$$

for the one-dimensional interface [$d=m=1$; see Eq. (153) for generic d and m]. It is the temperature at which the intermediate lengthscales r_0 and r_1 collapse—we recall that r_1 marks the end of the thermal regime while r_0 marks the beginning of the RM regime, see Fig. 8. Strikingly, the same T_c holds for the interface (73) and the toy model in Eq. (136). Moreover, in their corresponding variational computation T_c separates the two regimes for the RSB cutoff in $[\sigma](u)$, that is, corresponds to having the parameter $\tilde{A}$ of order unity, see Eqs. (48) and (112). The generic scaling arguments of Sec. VI indicate it is certainly no coincidence that these criteria, albeit disparate, in fact all lead to the same T_c.

Let's now depict each of the temperature regime, having in mind to compare our two models at hand (the results are summarized in Fig. 8). (i) The *high-temperature regime* $T \gg T_c$ is characterized by the existence of only two roughness regimes, the thermal and the RM ones, which connect at a lengthscale $r_* \sim \frac{T^5}{cD^2}$ common to both GVMs [see Eqs. (75) and (137)]. We have seen in Sec. VI how this unique ξ-independent length r_* was imposed by the Hamiltonian generic scaling properties, independently of the actual values of the asymptotic exponent ζ_{RM}. For $r<r_*$, $B(r)\sim Tr$ is thermal, disorder plays no role and thermal fluctuations enhance roughness. On the other hand, for $r>r_*$ the roughness scales as $B(r)\sim T^{2\hat{p}}r^{2\zeta_{\text{RM}}}$, meaning that it now *decreases* as temperature increases ($\hat{p}=-\frac{1}{3}$ by scaling, see also Refs. 28, 29, and 49)—physically, it means that thermal fluctuations inhibit the interface excursions to spread too widely in the random potential. We also remark that for the toy model, the roughness and thorn exponent obtained by GVM are the exact ones ($\zeta_{\text{RM}}=\frac{2}{3}$, $\hat{p}_{\text{RM}}=-\frac{1}{3}$) while for the interface one gets $\zeta_{\text{asympt}}=\frac{3}{5}$ and $\hat{p}_{\text{RM}}=0$. In the high temperature regime the rounded toy model, coupled to the GVM, thus provides a reasonable description of the interface and its crossovers. It is a more efficient mapping than to use directly the GVM on the variational Hamiltonian. (ii) In the *low-temperature regime* $T \ll T_c$, ξ becomes relevant and two lengthscales r_0 and r_1 now define an intermediate regime separating the thermal and RM ones. The GVM has allowed us to compute the actual crossover function of the roughness in Eqs. (82) and (83), versus Eq. (133). It is instructive to compare the value of r_0 to the Larkin length L_c obtained in the Larkin model or through FRG. Using, for instance, the notation of Ref. 31 [Eq. (4.17) with the random force strength $\Delta(0)=D\xi^{-3}$ and the disorder correlation length $r_f=\xi$] one has

$$L_c \sim \left(\frac{c^2\xi^2}{D\xi^{-3}}\right)^{1/3} \sim \left(\frac{c^2\xi^5}{D}\right)^{1/3}, \tag{155}$$

which matches exactly the low-temperature limit result in Eq. (64) $r_0 \sim \xi^{5/3}c^{2/3}D^{-1/3}$ for the 1D interface. On the other hand, the toy model exhibits a different scaling $r_0 \sim \xi^{3/2}cD^{-1/2}T^{1/2}$, see Eq. (128). In the low-temperature regime, the direct GVM results for the full 1D interface provide a better picture than the use of the rounded toy model. We can thus use whatever mapping is more appropriate depending on the temperature regime we are interested in.

Let us emphasize that depending on their order, the limits $\xi \to 0$ and $T \to 0$ lead to different physical regimes, since T_c crucially depends on ξ. The question of determining whether experimentally one lies in the low- or high-temperature regime is thus of particular interest, and is discussed in Sec. VII B. Note that on the numerical side, the high-T regime can be probed through the directed polymer[29] for which the roughness rescales as in Eq. (152).

It is also instructive to inspect the zero-temperature limit in detail: on the one hand the toy model has again the correct $\zeta_{\text{RM}}=\frac{2}{3}$ but since $\hat{p}^{\text{toy}}_{\text{RM}}<0$ the toy model also predicts a nonphysical divergence of $B(r)$ as $T \to 0$ in the random manifold regime, although the roughness should remain finite and not depend on T, as predicted, e.g., from the FRG zero-temperature fixed point.[31] One may conjecture that the behavior $B(r)\sim T^{-2/3}r^{4/3}$ remains valid for $r>r_\star$ only for a finite range of temperature, below which the scaling would become $B(r)\sim T^0 r^{4/3}$ with an effective thorn exponent $\hat{p}_{\text{RM}}=0$. To describe this behavior in the toy model approach, one would need to introduce a large scale cutoff (possibly *not* being the system size) to prevent the roughness to diverge in the limit $T \to 0$.

B. Consequences for the dynamics: The quasistatic creep regime

Although satisfactory from a theoretical point of view, the determination of the crossover lengths r_0 and r_1 may not yield directly observable predictions since in many instances the experimental resolution for $B(r)$ is insufficient to probe such small lengthscales. A context however where an indirect measurement could be achieved is that of interfaces driven by a small force F (compared to the "depinning" force F_c). Instead of following a mere linear response, the velocity $v(F)$ of the interface is given by the "creep law,"[22,31,50,51] archetypal of glassy systems[13,52]

$$v(F) \sim \exp\left[-\beta U_c \left(\frac{F_c}{F}\right)^{\mu}\right], \tag{156}$$

where $\mu = \frac{d-2+2\zeta}{2-\zeta}$ is the creep exponent, $F_c = c\xi/L_c^2$ is a characteristic depinning force and $U_c = c\xi^2/L_c$ an energy scale (see Ref. 52 for a review). In the previous expressions, ξ represents the effective width of the interface, and its value depends on whether one lies in the low- or high-temperature regime—which is in general not known in practice. A way to discriminate between the two regimes is to use U_c itself (readily attainable when fitting the creep law in Eq. (156) on numerical or experimental data) since its c, D, T dependence is directly related to that of the width ξ and of the Larkin length L_c.

In the high-temperature regime, taking $U_c = c\xi_{\rm eff}^2/r_*$ directly leads to a linear behavior $U_c = T$, a result at first sight compatible, e.g., with the numerical simulations of Ref. 53, where the measured value of U_c is indeed proportional to T. However, the value of F_c used in Ref. 53 is the zero-temperature critical depinning force, not scaling such as the characteristic force $F_c = c\xi_{\rm eff}/r_*^2 = c^2 D^3 T^{-7}$. The interpretation of the temperature dependence of U_c observed in numerical models thus remains to be clarified.

In the low-temperature regime, one has $U_c = c\xi^2/L_c$ where ξ is the microscopic width of the interface, and L_c is given by Eq. (155). This yields $U_c = (\xi c D)^{1/3} = T_c$ which is now temperature independent. In experiments on magnetic domain walls in ultrathin ferromagnetic films with perpendicular anisotropy,[1,2,54] which are thought to be possible experimental realizations of a 1D interface with short-range elasticity and random-bond disorder (precisely the case we have studied in this paper), quantities such as the roughness or the response to small force have been measured, and a question is to determine whether the low-temperature regime of our model may describe these results. Before examining this, we first point out a possible caveat: it is not clear whether the interface is at equilibrium or not; though the measured roughness $\zeta_{\rm RM} \approx 0.66$ is compatible with the theoretical value $\zeta_{\rm RM} = \frac{2}{3}$, it could also be that the interface is stuck in a very slowly relaxing state, reached due to the applied external field. In that case, the measured depinning roughness exponent is also compatible with the result $\zeta^{\rm dep} \approx 0.63$ for an interface with harmonic $(\nabla_z u)^2$ and non-harmonic $(\nabla_z u)^4$ contributions[55] (this value of $\zeta^{\rm dep}$ is more relevant for experiments than the ill-defined result $\zeta^{\rm dep} \approx 1.2$ of the purely harmonic elasticity).

Assuming nevertheless that the interface observed in those experiments is at equilibrium we can examine whether the analysis we have put forward applies. A first evidence that experiments on magnetic DW fall into the low-T regime is that the observed value of U/T actually depends on the combination of c and ξ (see e.g., Table I in Ref. 2, where U/T is denoted $T_{\rm dep}/T$) as opposite to high-T behavior $U_c = T$. In another experiment on magnetic DWs,[54] one can estimate T_c from the elastic constant $c \simeq 2.4 \times 10^{-12}$ J m^{-1}, the domain wall width $\xi \simeq 8$ nm and the Larkin length $L_c \simeq 40$ nm (estimated from small force measurements). Using our expressions to compute T_c, one arrives at $T_c \simeq 325$ K which is indeed slightly above the room temperature $T \simeq 300$ K of the experiment, suggesting that the interface is indeed in the low-temperature regime. Further evidence could be provided by a direct evaluation of $p_{\rm RM}$ which should be zero in that case.

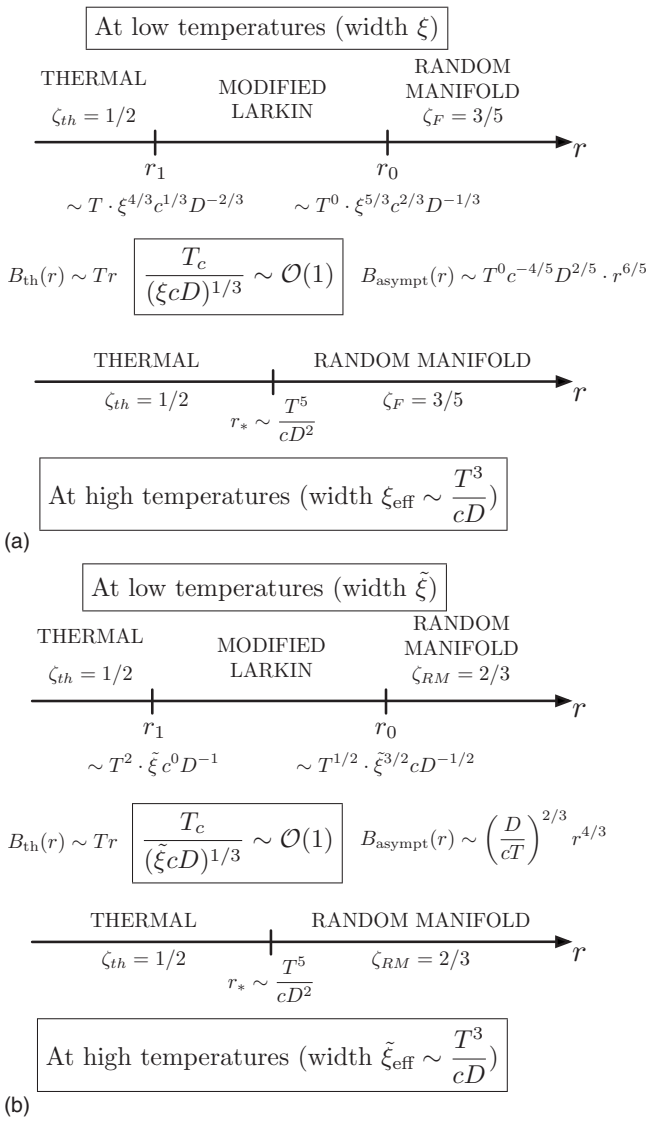

FIG. 8. Summary of the GVM predictions for (a) the 1D interface and (b) the toy-model roughness about their roughness regimes and their crossover lengthscales, at low versus high temperatures.

VIII. CONCLUSION

In this paper we have examined the static roughness of a one-dimensional interface subjected to a random-bond disorder. Using a Gaussian variational method we have determined the various regimes due to the finite width ξ of the interface (or equivalently to the finite correlation length of the disorder). We obtained that at large temperature, there is one universal ξ-independent crossover length from small to large lengthscales regimes, whereas at low temperature two ξ-dependent crossover lengths describe a more complex intermediate regime. Results summarized in Fig. 8(a) and

show that the low-temperature regime is correctly tackled only if one keeps ξ finite.

To discuss the scaling of the different roughness regimes, we have compared the results on the original model with the ones on a modified "rounded" toy model, which happens to capture the correct random-manifold exponent but turns out to be ill-defined in the $T \to 0$ limit. The high-temperature results match those of the interface, while at low T the scalings of the intermediate lengths differ, due to a distinct RM exponent—see Fig. 8(b) for a summary.

We have described the existence of two temperature regimes above and below a characteristic temperature $T_c = (\xi c D)^{1/3}$. On the numerical side simulations[29] show for the directed polymer clear evidence supporting the existence of a high-temperature regime with $B(r) \sim T^{2\beta} r^{2\zeta_{\mathrm{RM}}}$ with $\beta = -\frac{1}{3}$. However the observation on the experimental side of a negative thorn exponent β or of a T-dependent Larkin length remains to be done. One first question would be to know whether the temperature T_c is physically relevant or not. We have estimated that in creep experiments on magnetic DWs, the value of T_c is above, but of the order of T, and it would be interesting to clarify this question, e.g., by a direct measurement of β in both regimes.

The analysis we have presented also raises several interesting questions and suggests extensions deserving further inquest: one can wonder to what extent the variational method induces artifacts in the crossover lengthscales scalings we put forward, and try to investigate this question by use of the FRG, tackling in particular the low- and high-temperature regimes—in other words, one would need to reconcile the zero-temperature fixed point with the observed T dependence. On the other hand, the modified toy model proved to be an attractive simpler version of the problem, rich enough to encompass many correct scalings of the interface, except for the $T \to 0$ limit. One could for instance refine the toy model by introducing a large-scale cutoff that would constrain the roughness to remain finite in this limit. An exact rather than GVM solution may also be attainable. Finally, given the success of this model in describing the static properties, it would be interesting to ascertain how much the dynamics of the interface could be fairly approximated by the Langevin dynamics corresponding to the rounded toy model.

ACKNOWLEDGMENTS

We would like to thank Sebastian Bustingorry, Alejandro Kolton, Pierre Le Doussal, Markus Müller, Alberto Rosso, and Valerii M. Vinokur for interesting discussions. T.G. would like to thank KITP, where the final part of this work was done, and NSF under Grant No. NSF PHY05-51164 for support. This work was supported in part by the Swiss NSF under MaNEP and Division II.

APPENDIX A: "FLORY-TYPE" SCALING ARGUMENTS

Simple back-of-the-napkin power-counting leads to the so-called Flory (or Imry-Ma) estimation for the roughness exponent: this is what we relate in that appendix, for the interface and for its toy model. Assuming that at distance $z=L$ the interface presents typical excursions of extension $u=u(L)$ in the transverse direction, we write that the elastic and disorder contributions to the Hamiltonian scale according to[33]

$$\mathcal{H}_{\mathrm{el}}[u] = \frac{c}{2}\int_{\mathbb{R}} dz \cdot [\nabla_z u(z)]^2 \sim L^{d-2}u^2, \tag{A1}$$

$$\mathcal{H}_{\mathrm{dis}}[u,\tilde{V}] = \int_{\mathbb{R}} dz \cdot \tilde{V}[z,u(z)] \sim L^{d/2}u^{-m/2}, \tag{A2}$$

where we have used that $\overline{\tilde{V}(z,x)\tilde{V}(z',x')} = \delta^{(d)}(z-z') R_\xi(x-x') \sim L^{-d}u^{-m}$ to determine the scaling of $\tilde{V}$. Assuming that in the RM regime both contributions scale in the same way $\mathcal{H}_{\mathrm{el}} \sim \mathcal{H}_{\mathrm{dis}}$, we obtain

$$u(L) \sim L^{\zeta_F}, \quad \zeta_F = \frac{4-d}{4+m}. \tag{A3}$$

We analyze in Sec. VI why this Flory-type argument does not yield the correct RM exponent (e.g., $\zeta_F = 3/5$ instead of $\zeta_{\mathrm{RM}} = 2/3$ for the 1D interface). It is instructive to observe that on the contrary the same argument actually *works* for the toy model of Sec. V. Assuming now that the end point of the directed polymer $y(t)$ has excursions of order Y at time t, one gets the following scaling for the contributions to the effective free-energy in Eq. (89)

$$F_{\mathrm{el}}(y,t) = \frac{c}{2t}y^2 \sim t^{-1}Y^2, \tag{A4}$$

$$F_{\mathrm{dis}}(y) = \int_0^y dy' \cdot \eta(y') \sim Y^{1/2}, \tag{A5}$$

where we have used that $\overline{\eta(y)\eta(y')} = \tilde{D} \cdot R_{\tilde{\xi}}(y-y') \sim Y^{-1}$ to determine the scaling of η. Imposing $F_{\mathrm{el}} \sim F_{\mathrm{dis}}$ one obtains

$$Y \sim t^{\zeta_F^{\mathrm{toy}}}, \quad \zeta_F^{\mathrm{toy}} = \frac{2}{3}. \tag{A6}$$

APPENDIX B: HIERARCHICAL MATRICES

In this appendix we recall some properties of the hierarchical matrices. Both to fix the notations and for convenience for the reader we also give the inversion formulas of replica-symmetric (RS) and full-replica-symmetry-breaking (full-RSB) Ansatz directly in the limit $n \to 0$, using extensively the formulas and derivations of Mézard and Parisi in Refs. 33 and 35.

The replica trick constrains the structure of the $n \times n$ matrix G^{-1}_{ab} which must be symmetric and equivalent under permutation over the replica indices. The matrix has to be inverted in the limit $n \to 0$. A hierarchical matrix can be reconstructed by all the permutations of its first line, which can be chosen as the reference sequence in which the coefficients are classified monotonously. Such a generic $n \times n$ matrix $\hat{G}$ and its corresponding inverse matrix $\hat{G}^{-1}$ (also hierarchical) are thus defined by

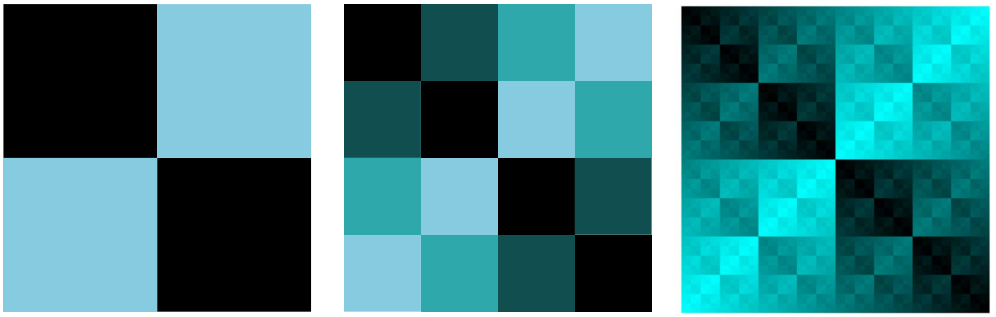

FIG. 9. (Color online) Examples of hierarchical matrices of $n \times n$ blocks with increasing integer k of replica-symmetry breaking. Each shade of color corresponds to a different value for the coefficients of the matrices.

$$\hat{G} \equiv \begin{pmatrix} \tilde{G} & & G_{a\neq b} \\ & \ddots & \\ G_{a\neq b} & & \tilde{G} \end{pmatrix} \Leftrightarrow \hat{G}^{-1} \equiv \begin{pmatrix} \tilde{G}^{-1} & & G^{-1}_{a\neq b} \\ & \ddots & \\ G^{-1}_{a\neq b} & & \tilde{G}^{-1} \end{pmatrix} \tag{B1}$$

or in the more compact way

$$\hat{G} \equiv \left(\tilde{G}, G_{a\neq b}\right) \Leftrightarrow \hat{G}^{-1} \equiv \left(\tilde{G}^{-1}, G^{-1}_{a\neq b}\right), \tag{B2}$$

where $G_{aa}=\tilde{G}$ and $G^{-1}_{aa}=\tilde{G}^{-1}$ $\forall a$.

This allows the definition of the *connected* part of these matrices, i.e., the sum of the coefficients on any line or column $G_c=\Sigma_a G_{ab}=\Sigma_b G_{ab}$, a conserved quantity which satisfies for two inverse matrices the relation

$$G_c G_c^{-1} = 1. \tag{B3}$$

The simplest case of a hierarchical matrix is the RS Ansatz, in which all the off-diagonal coefficients of the matrix are equal

$$\hat{G}^{-1} \equiv \left(\tilde{G}^{-1}, G^{-1}\right) \Leftrightarrow \hat{G} \equiv \left(\tilde{G}, G\right) \tag{B4}$$

and in the limit $n \to 0$

$$G_c^{-1} \equiv \tilde{G}^{-1} - G^{-1}, \quad G_c \equiv \tilde{G} - G,$$

$$G = -\frac{G^{-1}}{(G_c^{-1})^2}, \quad \tilde{G} = \frac{1}{G_c^{-1}}\left(1 - \frac{G^{-1}}{G_c^{-1}}\right). \tag{B5}$$

If the off-diagonal terms count at least two different values $\{g_0, \ldots, g_k\}$, we have a RSB Ansatz, the integer k counting the number of such breakings (see Fig. 9 for generic examples of this structure). The integer n being arbitrarily large, in the limit $k \to \infty$ the monotonous sequence of coefficients on the first line of the matrix is more adequately described by a monotonous function $G(u)$, depending on a mapping parameter $u \in [0,1]$. Thus a *full RSB* hierarchical matrix is defined by

$$\hat{G} = \left(\tilde{G}, G(u)\right) \text{ with } u \in [0,1]. \tag{B6}$$

The full-RSB Ansatz is actually the most generic description of a hierarchical matrix (in regards to the limit $n \to 0$) since the replica-symmetric and k-RSB Ansatz can be recovered using step functions for $G(u)$. The peculiar symmetries of hierarchical matrices allow to determine generic inversion formulas directly in the limit $n \to 0$,[33] once the first line of the matrix is given. Thereafter they have been adapted to the following definition of full-RSB hierarchical matrices:

$$\hat{G}^{-1}(q) \equiv \left(G_c^{-1} - \tilde{\sigma}, -\sigma(u)\right) \Leftrightarrow \hat{G}(q) \equiv \left(\tilde{G}(q), G(q,u)\right) \tag{B7}$$

$\sigma(u)$ being defined as a monotonous function on the interval $[0,1]$, the discrete sums of matrix operations are replaced by integrals. Note that the definition of the connected part G_c^{-1} implies that

$$\tilde{\sigma} = -\int_0^1 du \cdot \sigma(u). \tag{B8}$$

We define the following self-energy, illustrated in Fig. 10:

$$[\sigma](u) \equiv u \cdot \sigma(u) - \int_0^u dv \cdot \sigma(v). \tag{B9}$$

This definition implies in particular that $[\sigma]'(u) = u \cdot \sigma'(u)$.

This self-energy acts in fact as a mass term in the propagators of the following inversion formulas:

$$\tilde{G} = \frac{1}{G_c^{-1}}\left(1 + \int_0^1 \frac{dv}{v^2} \frac{[\sigma](v)}{G_c^{-1} + [\sigma](v)} + \frac{\sigma(0)}{G_c^{-1}}\right), \tag{B10}$$

$$\tilde{G} - G(u) = \frac{1}{u} \frac{1}{G_c^{-1} + [\sigma](u)} - \int_u^1 \frac{dv}{v^2} \frac{1}{G_c^{-1} + [\sigma](v)}, \tag{B11}$$

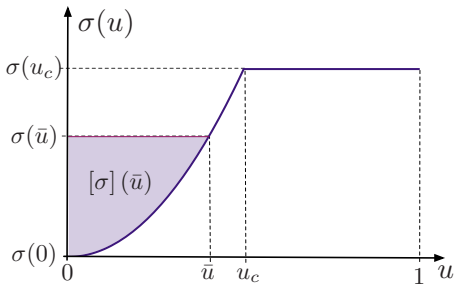

FIG. 10. (Color online) The mass term $[\sigma](\bar{u})$ corresponds to the shaded area between $\sigma(\bar{u})$ and the $\sigma(u)$ curve, and thus saturates at the cutoff $u=u_c$.

$$\tilde{G} - G(u) = \frac{1}{G_c^{-1} + [\sigma](1)} + \int_u^1 dv \frac{\sigma'(v)}{[G_c^{-1} + [\sigma](v)]^2}. \tag{B12}$$

The relation (B12) can be obtained from Eq. (B11) by a simple integration by parts.

From the full-RSB point of view the RS Ansatz is the particular case when $\sigma(u)$ is a constant

$$\sigma(u) = \sigma_0 \; \forall \; u \in [0,1] \Rightarrow [\sigma](u) = 0 \; \forall \; u \in [0,1] \tag{B13}$$

in which case the previous inversion formulas collapse indeed on the RS case in Eq. (B5).

In the context of a GVM in a Fourier-space representation (as the one described in Sec. III), those inversion formulas have still to be integrated over the Fourier modes q in order to deal with the saddle-point equation or the computation of the roughness. Inverting conveniently the order of integration over the Fourier modes and over the RSB parameter u, and pushing the ultraviolet cutoff to ∞, the following identities for propagators are useful ($A > 0$ is typically a self-energy $[\sigma](u)$) for the case of a 1D interface:

$$\int_{\mathbb{R}} đq \frac{1}{cq^2 + A} = \frac{A^{-1/2}}{2\sqrt{c}}, \tag{B14}$$

$$\int_{\mathbb{R}} đq \frac{1}{(cq^2 + A)^2} = \frac{A^{-3/2}}{4\sqrt{c}} \tag{B15}$$

and

$$\int_{\mathbb{R}} đq \frac{2[1 - \cos(qr)]}{cq^2(cq^2 + A)} = \frac{1}{A\sqrt{Ac}}(e^{-\sqrt{A/c}\cdot r} - 1 + \sqrt{A/c} \cdot r) = \frac{1}{A\sqrt{Ac}} \sum_{k=2}^{\infty} \frac{(-\sqrt{A/c} \cdot r)^k}{k!} \tag{B16}$$

at first for $\int_{\mathbb{R}} đq[\tilde{G}(q) - G(q,u)]$ in the manipulation of the saddle-point equation and second for $\int_{\mathbb{R}} đq[1 - \cos(qr)]\tilde{G}(q)$ in the computation of the roughness.

For the sake of completeness here is finally the formula for the trace of hierarchical matrices in the limit $n \to 0$, adapted from Sec. AII11 of Ref. 33 to our conventions [with $[G](u)$ being defined similarly to $[\sigma](u)$ in Eq. (B9)]

$$\lim_{n\to 0} \frac{1}{n} \mathrm{Tr} \log \hat{G}^{-1} = \log(G_c^{-1}) - \frac{\sigma(0)}{G_c^{-1}} - \int_0^1 \frac{du}{u^2} \log\left[\frac{G_c^{-1} + [\sigma](u)}{G_c^{-1}}\right], \tag{B17}$$

$$\lim_{n\to 0} \frac{1}{n} \mathrm{Tr} \log \hat{G} = \log(G_c) + \frac{G(0)}{G_c} - \int_0^1 \frac{du}{u^2} \log\left[\frac{G_c - [G](u)}{G_c}\right]. \tag{B18}$$

The quantity $\frac{1}{n}\mathrm{Tr} \log \hat{G}$ is actually to be used in the GVM for the computation of the free energies $\mathcal{F}_0$ and $\mathcal{F}_{\mathrm{var}}$ associated to a trial Hamiltonian $\mathcal{H}_0$, see Appendix C in Ref. 32 for an example.

*elisabeth.agoritsas@unige.ch

[1] S. Lemerle, J. Ferré, C. Chappert, V. Mathet, T. Giamarchi, and P. Le Doussal, Phys. Rev. Lett. **80**, 849 (1998).
[2] P. J. Metaxas, J. P. Jamet, A. Mougin, M. Cormier, J. Ferré, V. Baltz, B. Rodmacq, B. Dieny, and R. L. Stamps, Phys. Rev. Lett. **99**, 217208 (2007).
[3] T. Tybell, P. Paruch, T. Giamarchi, and J.-M. Triscone, Phys. Rev. Lett. **89**, 097601 (2002).
[4] P. Paruch, T. Giamarchi, and J.-M. Triscone, Phys. Rev. Lett. **94**, 197601 (2005).
[5] J. Krim and G. Palasantzas, Int. J. Mod. Phys. B **9**, 599 (1995).
[6] S. Moulinet, C. Guthmann, and E. Rolley, Eur. Phys. J. E. **8**, 437 (2002).
[7] P. Le Doussal, K. J. Wiese, S. Moulinet, and E. Rolley, EPL **87**, 56001 (2009).
[8] M. Alava and K. Niskanen, Rep. Prog. Phys. **69**, 669 (2006).
[9] M. Kardar, Phys. Rep. **301**, 85 (1998).
[10] T. Giamarchi and P. Le Doussal, *Statics and Dynamics of Disordered Elastic Systems* (World Scientific, Singapore, 1998), p. 321.
[11] G. Grüner, Rev. Mod. Phys. **60**, 1129 (1988).
[12] S. Brazovskii and T. Nattermann, Adv. Phys. **53**, 177 (2004).
[13] G. Blatter, M. V. Feigel'man, V. B. Geshkenbein, A. I. Larkin, and V. M. Vinokur, Rev. Mod. Phys. **66**, 1125 (1994).
[14] A.-L. Barabàsi and H. E. Stanley, *Fractal Concepts in Surface Growth* (Cambridge University Press, Cambridge, 1995).
[15] T. Halpin-Healy and Y.-C. Zhang, Phys. Rep. **254**, 215 (1995).
[16] G. Giacomin, *Random Polymer Models* (Imperial College Press, London, 2007).
[17] D. Forster, D. R. Nelson, and M. J. Stephen, Phys. Rev. A **16**, 732 (1977).
[18] J. Burgers, *The Nonlinear Diffusion Equation* (Reidel, Boston, 1974).
[19] M. Kardar, Nucl. Phys. B **290**, 582 (1987).
[20] M. Kardar, G. Parisi, and Y.-C. Zhang, Phys. Rev. Lett. **56**, 889 (1986).
[21] M. Kardar and Y.-C. Zhang, Phys. Rev. Lett. **58**, 2087 (1987).
[22] L. B. Ioffe and V. M. Vinokur, J. Phys. C **20**, 6149 (1987).
[23] D. A. Huse, C. L. Henley, and D. S. Fisher, Phys. Rev. Lett. **55**, 2924 (1985).
[24] M. Balázs, J. Quastel, and T. Seppäläinen, arXiv:0909.4816 (unpublished).
[25] T. Sasamoto and H. Spohn, Nucl. Phys. B **834**, 523 (2010).
[26] G. Amir, I. Corwin, and J. Quastel, Commun, Pure Appl. Math. (to be published); arXiv:1003.0443.
[27] V. Dotsenko, EPL **90**, 20003 (2010).
[28] P. Calabrese, P. Le Doussal, and A. Rosso, EPL **90**, 20002 (2010).

[29] S. Bustingorry, P. Le Doussal, and A. Rosso, Phys. Rev. B **82**, 140201 (2010).
[30] D. S. Fisher, Phys. Rev. Lett. **56**, 1964 (1986).
[31] P. Chauve, T. Giamarchi, and P. Le Doussal, Phys. Rev. B **62**, 6241 (2000).
[32] T. Giamarchi and P. Le Doussal, Phys. Rev. B **52**, 1242 (1995).
[33] M. Mézard and G. Parisi, J. Phys. I **1**, 809 (1991).
[34] P. Le Doussal, M. Müller, and K. J. Wiese, Phys. Rev. B **77**, 064203 (2008).
[35] M. Mézard, G. Parisi, and M. A. Virasoro, *Spin Glass Theory and Beyond*, World Scientific Lecture Notes in Physics (World Scientific, Singapore, 1987), Vol. 9.
[36] H. Yoshino, J. Phys. A **29**, 1421 (1996).
[37] S. Bustingorry, A. B. Kolton, and T. Giamarchi, EPL **81**, 26005 (2008).
[38] E. Medina and M. Kardar, Phys. Rev. B **46**, 9984 (1992).
[39] E. B. U. Schulz, J. Villain, and H. Orland, J. Stat. Phys. **51**, 1 (1988).
[40] T. Hwa and D. S. Fisher, Phys. Rev. B **49**, 3136 (1994).
[41] D. S. Fisher and D. A. Huse, Phys. Rev. B **43**, 10728 (1991).
[42] I. Larkin, Sov. Phys. JETP **31**, 784 (1970).
[43] V. Dotsenko, V. Geshkenbein, D. Gorokhov, and G. Blatter, arXiv:1007.0852 (unpublished).
[44] M. Mézard, J. Phys. (France) **51**, 1831 (1990).
[45] G. Parisi, J. Phys. (France) **51**, 1595 (1990).
[46] J. Bouchaud and H. Orland, J. Stat. Phys. **61**, 877 (1990).
[47] P. Le Doussal and C. Monthus, Physica A **317**, 140 (2003).
[48] M. Mézard and G. Parisi, J. Phys. I France **2**, 2231 (1992).
[49] T. Nattermann, Y. Shapir, and I. Vilfan, Phys. Rev. B **42**, 8577 (1990).
[50] M. V. Feigel'man, V. B. Geshkenbein, A. I. Larkin, and V. M. Vinokur, Phys. Rev. Lett. **63**, 2303 (1989).
[51] T. Nattermann, Phys. Rev. Lett. **64**, 2454 (1990).
[52] T. Giamarchi, A. B. Kolton, and A. Rosso, Lect. Notes Phys. **688**, 91 (2006).
[53] A. B. Kolton, A. Rosso, and T. Giamarchi, Phys. Rev. Lett. **94**, 047002 (2005).
[54] V. Repain, M. Bauer, J.-P. Jamet, J. Ferré, A. Mougin, C. Chappert, and H. Bernas, EPL **68**, 460 (2004).
[55] A. B. Kolton, A. Rosso, T. Giamarchi, and W. Krauth, Phys. Rev. B **79**, 184207 (2009).